Aus der Universitätsklinik für Zahn-, Mund- und Kieferheilkunde
Tübingen

Abteilung Klinik und Poliklinik für Mund-, Kiefer- und
Gesichtschirurgie

Ärztlicher Direktor: Professor Dr. Dr. S. Reinert

Chronic Inflammation of the Oral Cavity and Squamous Cell DNA Methylation

Inaugural-Dissertation
zur Erlangung des Doktorgrades
der Zahnheilkunde

der Medizinischen Fakultät
der Eberhard Karls Universität
zu Tübingen

vorgelegt von
Jacqueline Anke Katja Gasche
aus
Wien

2010

Aus der Universitätsklinik für Zahn-, Mund- und Kieferheilkunde
Tübingen

Abteilung Klinik und Poliklinik für Mund-, Kiefer- und
Gesichtschirurgie

Ärztlicher Direktor: Professor Dr. Dr. S. Reinert

Chronic Inflammation of the Oral Cavity and Squamous Cell DNA Methylation

Inaugural-Dissertation
zur Erlangung des Doktorgrades
der Zahnheilkunde

der Medizinischen Fakultät
der Eberhard Karls Universität
zu Tübingen

vorgelegt von
Jacqueline Anke Katja Gasche
aus
Wien

2010

Dekan: Professor Dr. I. B. Autenrieth

1. Berichterstatter: Professor Dr. Dr. J. Hoffmann
2. Berichterstatter: Frau Professor Dr. K. Klingel

Table of Contents

1 Introduction

1.1 Clinical Background on Oral Squamous Cell Carcinoma

Oral squamous cell carcinoma (OSCC) was ranked as the ninth most frequent cancer worldwide in 2002 accounting for more than 100,000 deaths per year. (Subbalekha et al., 2008; Sturgis et al., 2004) OSCC is twice more common in men than in women. (Parkin et al., 1999) It is a multifactorial disease primarily associated with chronic tobacco and alcohol use, but also chronic inflammation, viral infections (Human Papillomavirus) and genetic predisposition. (Choi and Myers, 2008; Baez, 2008) As co-factors, betel nut chewing (in Asia), Shammah smokeless tobacco (in Arabia), candidiasis, diabetes, and dental plaque are known to contribute to oral tumorigenesis. (Bagan and Scully, 2008) The countries with the highest documented incidence rates directly reflect the prevalence of local habits: tobacco and alcohol are considered the main risk factors for OSCC in Europe and South Africa, while betel quid chewing causes high incidence rates in South-central Asia and Melanesia. The high incidence in Australia can be explained by the UV irradiation causing lip cancer. (Parkin et al., 1999)

Clinically, OSCC will usually appear as a non-healing ulcer, grow slowly and be asymptomatic. Potentially malignant lesions such as leukoplakia, erythroplakia, oral lichen planus and oral submucous fibrosis can result in tumorigenesis. (Mithani et al., 2007) The clinical detection is often problematic, as the tumor can present itself in a variety of clinical appearances. For staging purposes, the Union Internationale Contre le Cancer introduced the TNM-Classification (T-primary tumor size; N-regional lymph nodes; M-distant metastasis) which is now internationally used.

Therapy with curative intent consists of extensive surgery (mostly with neck dissection), adjuvant radio- and chemotherapy and complex reconstructive surgery. (Oliveira et al., 2008) As a complication, surgery may cause wound

infections resulting in functional morbidity, poor esthetic appeal and extended hospitalization. (Scully and Bagan, 2008) Yet, the surgical approach is preferred to non-surgical treatment due to its superior outcome in terms of overall survival rate and disease-free-time. (Scully and Bagan, 2008) An additional difficulty in the treatment of OSCC lies in the patient's decreased quality of life due to the reduced oral function and radiotherapy-induced xerostomia which leaves the oral cavity defenseless to caries, oral infections and halitosis.

Despite a multimodal surgical therapy, patients suffering from OSCC show a high incidence in relapse and death. (Choi and Myers, 2008) The 5-year-overall survival rate is estimated to approximately 60%, however only 5% improvement was achieved over the past 25 years. (Jemal et al., 2009) The concept of "Field Cancerization" is a probable reason for this high incidence in relapse or additional primary tumors, which might possibly be obviated by chemoprevention. (Thomson, 2002)

In order to improve therapy and survival statistics, it is essential to further explore the fundamental biology of OSCC and the dynamics leading to its progression.

1.2 Genetics and Epigenetics of Oral Squamous Cell Carcinoma

All malignant tumors commonly show the six essential hallmarks of cancer as depicted in Figure 1. (Hanahan and Weinberg, 2000) The activation of intracellular messenger signaling and the lack of response to growth inhibitory signals results in uncontrolled autonomous tumor growth. By evading apoptosis, cells refuse to go into programmed cell death and telomere lengthening gives the cells the potential to replicate without limits. The domination of pro-angiogenic factors supports blood vessel proliferation supplying the tumor with much needed nutrition. Due to loss of function of cellular adhesion molecules such as E-cadherin, E-selectin, integrins, and CD44, single tumor cells can

leave the primary tissue and metastasize into neighboring and distant regions. (Hanahan and Weinberg, 2000; Mendes et al., 2009)

Figure 1   **The hallmarks of cancer.** Modified from (Hanahan and Weinberg, 2000). The figure depicts a brief representation of the six key players responsible for tumorigenesis.

The biological mechanisms specific for OSCC carcinogenesis include DNA deletions (e.g. 9p, 3p, 17p, 13q, 8p, 11q), loss of heterozygosity (LOH), microsatellite instability (MSI), mutations (e.g. p53), histone deacetylation, and silencing of tumor suppressor genes by promoter hypermethylation. (Choi and Myers, 2008; Ishida et al., 2005; Shintani et al., 2001; Nakahara et al., 2006) Figure 2 describes the stepwise progression from normal to dysplastic to cancerous oral mucosa distinguishing between early and late events in tumorigenesis. An accumulation of those genetic and epigenetic changes might result in tumorigenesis.
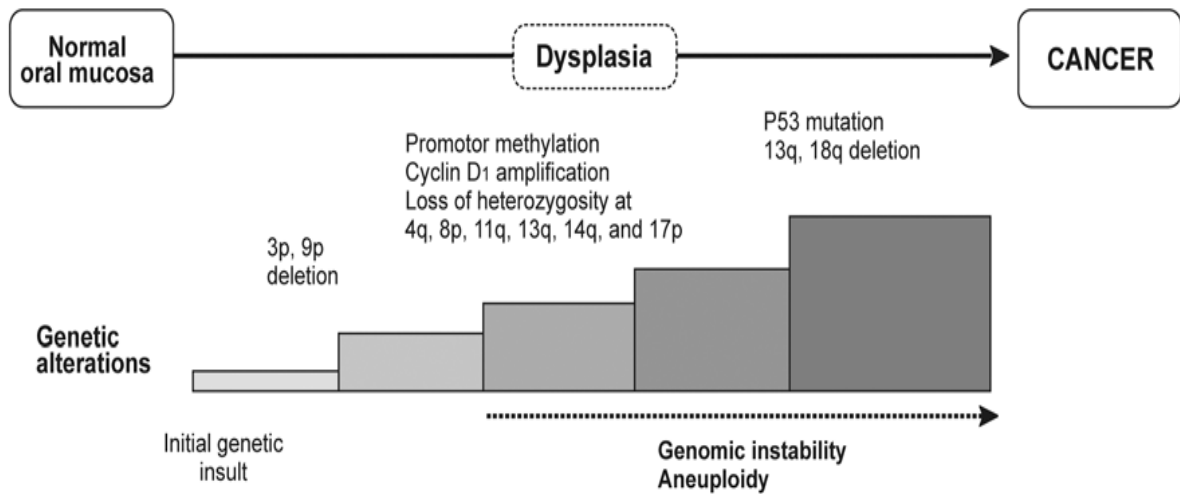
Figure 2 **Step by step tumor development of oral squamous cell carcinoma (OSCC).** Modified from (Choi and Myers, 2008). The figure describes genetic and epigenetic modifications distinguishing between early and late events leading to OSCC tumorigenesis.

Genetic changes typically manifest within the gene-encoding parts of the DNA directly affecting the genotype by variations within the DNA sequence. Loss of heterozygosity, microsatellite instability, point mutations and deletions are considered genetic changes. (Shaw, 2006)

Epigenetic changes altering gene expression occur without mutations of the DNA nucleotide sequence and may happen far more frequently than loss of gene function due to mutational events. (Viet and Schmidt, 2008) DNA methylation changes, histone modifications and recently also microRNAs are common epigenetic modulations of gene expression. (Esteller, 2002; Shaw, 2006; Schmezer and Plass, 2008)

In cancer, the two phenomena genome-wide hypomethylation and promoter hypermethylation often go hand in hand and play a pivotal role causing

chromosomal instability and transcriptional inactivation of tumor suppressor genes. (Yoo and Jones, 2006; Yang et al., 2004)

It has been proposed that DNA hypomethylation of repetitive elements contributes to tumorigenesis through chromosomal instability (CIN) leading to mitotic dysregulation and oncogene expression. (Choi et al., 2009) In OSCC, heterogenic karyotypes have been reported to cause dysregulation of the cell cycle and checkpoint controls. (Reshmi and Gollin, 2005) However, no published literature exists on the relation of hypomethylation and chromosomal instability as contributors to OSCC carcinogenesis.

LINE-1, long interspersed nucleotide element-1, is a repetitive DNA nucleotide sequence spread diffusely throughout the genome. Normally, DNA repetitive sequences are strongly methylated and make up about one third of the genome's total DNA methylation. A correlation between DNA repetitive element methylation and total genomic content of 5-methylcytosine has been observed. Therefore, LINE-1 has been suggested as surrogate marker for detecting the global methylation status. (Kim et al., 2009; Yang et al., 2004; Choi et al., 2009)

CpG hypermethylation is another key player in OSCC tumorigenesis and considered a rather early event. (Ha and Califano, 2006; Viet and Schmidt, 2008) Normal and premalignant tissues in the neighboring region of tumors frequently show signs of hypermethylation. (Ha and Califano, 2006) The chemical details of methylation are shown in Figure 3.
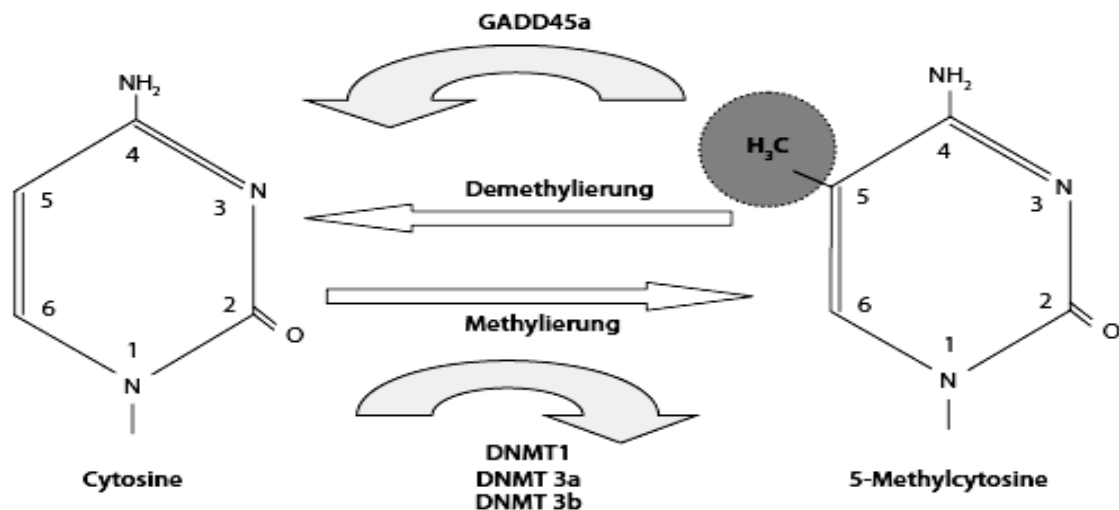
Figure 3 **DNA methylation.** The graph depicts the chemical structures of cytosine (left) and 5-methylcytosine (right). Several DNA methyltransferase (DNMT) enzymes cause methylation at position 5, while the enzyme GADD45a reverses it to a demethylated state. (Schmezer and Plass, 2008)

Hypermethylation occurs in the CpG islands, a cytosine-guanine-rich section located within 5'-untranslated regions of the promoter which may at times extend to the first exon. Aberrant promoter methylation occurs as a cytosine methylation at position 5 of the pyrimidin ring catalyzed by the enzyme DNA methyltransferase (DNMT), in which the methyl group is donated by S-Adenosyl-L-Methionine (SAM-e). (Schmezer and Plass, 2008; Yoo and Jones, 2006) The DNMT enzyme bends the cytosine ring out of the double helix and forms a complex with SAM-e. The SAM-e's methyl group is added to C5 of the cytosine ring and DNMT is released in a β-elimination reaction. (Yoo and Jones, 2006) There are three different DNA methyltransferases catalytically active in the human body: DNMT1, DNMT3a and DNMT3b. While DNMT1 is considered an enzyme that maintains pre-existing methylation, the function of DNMT3a and DNMT3b is primarily de novo methylation. (Esteller, 2002; Liu et al., 2008) The enzymatic activity of DNMTs is generally increased in tumors compared to normal tissue. (Esteller, 2002)

Hypermethylation of CpG islands is a common mechanism for gene inactivation. However, CpG island hypermethylation does not necessarily prove transcriptional silencing. Only dense hypermethylation will silence a gene. A positive cooperative effect has been observed supporting hypermethylation of multiple CpG islands until gene silencing is successfully achieved. (Esteller, 2002) Methylation within the promoter region interferes with transcription factors and inhibits their binding to the DNA. Therefore, the sequence cannot be transcribed and the gene is silenced although the genetic structure of a hypermethylated gene is still perfectly intact. Each tumor has its specific pattern of hypermethylated genes. (Shaw, 2006) Genes typically affected by hypermethylation are tumor suppressor genes, DNA repair genes, metastasis-associated genes, hormone receptor genes and angiogenesis-inhibiting genes. (Shaw, 2006) Several cellular pathways, such as the inactivation of DNA repair, cell cycle, apoptosis, cell adherence or carcinogen metabolism, are suspected to be affected by this mechanism. (Esteller, 2002; Hodge et al., 2005) As an example, hypermethylation could inactivate the gene encoding for the cell-to-cell adhesion molecule E-cadherin causing tumor invasiveness or it could inactivate the gene encoding for DAP (death associated protein) kinase resulting in cell immortalization. (Kudo et al., 2004; Shaw, 2006)

Aberrant DNA methylation is a reversible mechanism: either DNMTs can be blocked or methylation is reversed by the GADD45a enzyme. (Schmezer and Plass, 2008) Methylation is a dynamic process: Many gene loci that are hypermethylated in the primary tumor tissue can be found unmethylated in the corresponding metastasis. (Ha and Califano, 2006) Physiologically, genes are protected and if necessary repaired or stopped at the cell cycle checkpoints. Loss of function of tumor suppressor genes results in increased risk for mutability. Protection of CpG islands is provided by activators, histone acetyltransferases and the transcriptional machinery. On the contrary, hypermethylation can be induced by DNA methyltransferases, methyl-binding proteins (e.g. MeCP2), histone deacetylases, and transcriptional repressors. (Esteller, 2002)

Every individual develops its methylation pattern during early growth, which is usually maintained throughout life. During development, DNA methylation is a vital necessity and part of organ-specific cellular differentiation. In adults, the approximate 45,000 CpG islands distributed throughout the human genome are generally unmethylated. (Shaw, 2006) Physiological exceptions are long-term gene silencing by promoter hypermethylation of imprinted genes and the female X-chromosome. (Esteller, 2002; Shaw, 2006) With proceeding age, however, we commonly observe deviations from this methylation pattern. (Yoo and Jones, 2006; Yang et al., 2004) Aberrant hypermethylation of generally unmethylated CpG islands has been described in immortalized or transformed cells and is seen in close connection to transcriptional silencing of tumor suppressor genes existing in human cancer. (Herman et al., 1996) Aberrant methylation changes have generally been associated with aging, cancer, and other disease. (Yoo and Jones, 2006; Yang et al., 2004)

The majority of hypermethylated tumor types are located in the gastrointestinal tract (esophagus, stomach and colon). The exposure to external carcinogens might be the reason for this distribution implicating that also the oral cavity may be strongly affected. (Esteller, 2002) Commonly hypermethylated genes in head and neck squamous cell carcinoma (HNSCC) are TIMP3, ECAD, CDKN2A, MGMT, DAPK1, and RASSF1. (Schmezer and Plass, 2008) Aberrant DNA hypermethylation has also been seen in correlation with smoking habits in patients with HNSCC. (Schmezer and Plass, 2008)

As mentioned above, also histone modifications are considered epigenetic modifications. Histone modifications include acetylation, methylation, phosphorylation, ubiquitination, sumoylation, and biotinylation of the histone protein ends. (Schmezer and Plass, 2008) 147bp of DNA is wrapped around a histone protein octomer to form a complex called the nucleosome, the fundamental unit of the chromatin. (Yoo and Jones, 2006) Most posttranslational modifications occur at the amino-terminal tails of the histones

reaching out of the nucleosome. (Yoo and Jones, 2006) Deacetylation of the histones, catalyzed by the enzyme histone deacetylase (HDAC), gives them a positive charge. Attracted by the negative charged DNA, they will form a tight chromatin. The condensed chromatin is detained from binding transcription factors for gene expression; hence the gene will be silenced. For gene expression, the chemical structure has to return to a loose, acetylated configuration. (Shaw, 2006) A significant association between CpG hypermethylation and histone modification has been noticed. (Esteller, 2002; Ha and Califano, 2006; Shaw, 2006) While histone deacetylation is usually a reversible process, it seems irreversible in the presence of aberrant DNA hypermethylation. Hypermethylation changes the binding of histone complexes causing steady histone deacetylation. (Ha and Califano, 2006)

Also microRNAs (miRNA) can alter gene expression. They are small single-stranded RNA molecules approximately 22 nucleotides long not coding for any protein, but instead regulating numerous protein-encoding genes. (Kozaki et al., 2008; Park et al., 2009; Gomes and Gomez, 2008) In fact, it is believed that one single miRNA molecule can possibly control the expression of several hundreds of genes. (Schmezer and Plass, 2008; Park et al., 2009; Gomes and Gomez, 2008) With projected 1,000 miRNAs in the human genome, approximately one third of all messenger RNAs (mRNAs) might be posttranscriptionally regulated by miRNAs by blocking mRNA translation or degradation. (Park et al., 2009; Gomes and Gomez, 2008) The regulatory function of miRNAs includes cell growth, differentiation, apoptosis, and immune response. (Kozaki et al., 2008; Park et al., 2009) An overexpression of oncogenic miRNAs downregulates the expression of tumor-suppressor genes, while a decreased tumor-suppressor miRNA expression upregulates oncogenic proteins. (Gomes and Gomez, 2008) DNMTs have been proposed to be major targets of miRNAs closely linking DNA hypermethylation to miRNAs. Also, DNMT inhibitors can cause an overexpression of miRNAs. (Gomes and Gomez, 2008) Kozaki et al distinguished two miRNAs, miR-137 and miR-193a, out of a panel of 148 miRNAs, which were epigenetically silenced in OSCC tissues. An inverse

correlation between DNA methylation and these miRNAs was detected. (Kozaki et al., 2008) In another study, the saliva of OSCC patients showed a significantly decreased expression of miR-125a and miR-200a. (Park et al., 2009)

In epigenetics, aberrant DNA hypermethylation, histone modifications, and miRNAs go hand in hand mediating the human gene expression profile and contributing to OSCC tumorigenesis. (Schmezer and Plass, 2008)

1.3 Chronic Inflammation

Back in 1863, Rudolf Virchow was the first to hypothesize a link between inflammation and subsequent tumorigenesis. (Balkwill and Mantovani, 2001) To this day, the specific mechanisms of how chronic inflammation causes oral tumorigenesis are still not fully understood.

Chronic inflammation leading to tumor development seems like a paradox: Why would the host defense mechanism express an inflammatory response, when the tumor itself produces inflammatory factors apparently supporting tumorigenesis? (Balkwill and Mantovani, 2001) For long, the presence of inflammatory cells was thought to be the host's defensive response to premalignant lesions, but possibly inflammation could be part of the initiation process developing premalignant lesions and leading to tumorigenesis. (Bui and Schreiber, 2007) In the last decade, researchers found accumulating evidence that tumors are sustained or even encouraged by their inflammatory microenvironment. (Bromberg and Wang, 2009) While acute inflammation is seen as a valuable defense mechanism, chronic inflammation is considered a disease encouraging tumorigenesis. Chronic inflammation can be induced by various factors persistently stimulating the immune system. These factors may include infections of viral or bacterial origins and chemical irritants, which can endure for many years. (Hooper et al., 2009) Physiological inflammation, as we can find it for example during wound healing, is considered self-limiting. During

tumorigenesis, however, we see pathogenic dysregulation of the immune response without borders. (Coussens and Werb, 2002)

An acute inflammatory response launches with the recruitment of neutrophils and eosinophils. Monocytes migrate into the region of inflammation and transform into cytokine-producing macrophages. Also, mast cells release various inflammatory mediators including cytokines. Persisting chronic inflammation with increased oxidative stress has the potential to support neoplastic progression. Previous research has shown that especially macrophages, neutrophils, mast cells, eosinophils, and activated T-lymphocytes contribute to tumorigenesis. (Coussens and Werb, 2002)

Due to its constant exposure to the environment and its carcinogens, the oral cavity is particularly in danger to infections and inflammation. Chronic inflammation is considered a risk factor, which might promote genetic and epigenetic alterations leading to oral tumorigenesis. (Chakravarti et al., 2006; Whiteside, 2009) The mucosa and saliva present themselves as an immune cell-rich milieu creating a protective barrier against infectious agents. (Whiteside, 2009) However, poor oral hygiene, periodontal disease, and a microflora with an overgrowth of bacteria or *Candida* have shown a close association with an increased risk for tumorigenesis. Typically, the saliva of OSCC patients consists of higher concentrations of bacterial species compared to OSCC-free subjects. Chronic inflammation has been proposed as one of the possible pathways, by which various microorganisms like bacteria, fungus, and yeast might induce oral tumorigenesis. (Hooper et al., 2009) Leukoplakia, erythroplakia, lichen planus and oral submucous fibrosis are considered premalignant lesions, which bare the potential and highly-increased risk for OSCC development. (Nagpal and Das, 2003) In oral lichen planus and submucous fibrosis, an increased occurrence of inflammatory cells can be found, suggesting a close linkage of chronic oral inflammation and tumorigenesis. (Mithani et al., 2007; Rhodus et al., 2005)

From other tissues, we know that chronic bacterial infections and the host's inflammatory response may contribute to tumorigenesis. *Helicobacter pylori* cause inflammation of the gastric mucosa, which can further develop atrophy, metaplasia, dysplasia, and potentially degenerate into an adenocarcinoma. An infection with *Helicobacter pylori* causes the induction of cyclooxygenase (COX)-2 expression and an increase in neutrophils, phagocytes, and several proinflammatory cytokines within the gastric tissue. (Hooper et al., 2009) Interestingly, *Helicobacter pylori* infections causing gastric cancer involve IL-6 and STAT-3 pathways. (Coussens and Werb, 2002) In similar ways, *Porphyromonas gingivalis*, *Eikanella corrodens*, *Streptococcus anginosus*, and *Streptococcus mitis* are able to induce chronic inflammation and cause an increased production of inflammatory cytokines in the oral cavity. (Hooper et al., 2009)

Tumors are frequently surrounded by an inflammatory microenvironment, which actively promotes malignant cells. It is rich in inflammatory cytokines, growth factors, and chemokines. These factors are produced by the tumor itself and its surrounding mesenchymal tissue and contribute to malignant progression, invasion and metastasis. (Balkwill and Mantovani, 2001) Inflammatory cells evidently have major effects on neoplastic development contributing to tumor growth, genomic instability and angiogenesis. (Coussens and Werb, 2002) Inflammatory mediators, such as cytokines and chemokines, play an important role in tumor growth, maintenance, survival, migration, and the differentiation of the tumor microenvironment during tumorigenesis. (Coussens and Werb, 2002; Mendes et al., 2009) Also pro-inflammatory proteins, such as the inducible nitric oxide synthase (iNOS), vascular endothelial growth factor (VEGF) and COX-2, show a close affiliation to inflammation but also carcinogenesis. (Sappayatosok et al., 2009) COX-2, its prostaglandin products, and various other inflammatory factors have been detected at high levels in a variety of tumor tissues, including HNSCC. A COX-2 gradient was noticed increasing from hyperplasia to dysplasia with its highest expression in advanced malignancy. The isoenzyme COX-2 is only present under physiopathological conditions, for example, in the

presence of an inflammatory stimulus and often linked with neoplasia. High COX-2 levels are associated with increased cell proliferation, angiogenesis, invasiveness, inhibition of apoptosis, and immune surveillance. (Mendes et al., 2009) One study shows that patients with long-term aspirin or non-steroidal anti-inflammatory drugs (NSAIDs) treatment inhibiting COX have 40 to 50% less risk to develop colon cancer and may also prevent lung, esophageal, and gastric cancer. (Coussens and Werb, 2002) This observation suggests that inflammation might generally be a risk factor of tumorigenesis.

A distinct subgroup of OSCC with high levels of CpG promoter methylation was identified as the CpG island hypermethylation phenotype (CIMP). CIMP in oral neoplasia is association with an increased host inflammatory response, although the tumor appears less aggressive in terms of reduced tumor thickness, less nodal invasion and enhanced prognosis. This observation suggests the host inflammatory response to be a favorable prognostic factor in CIMP-associated OSCC. There are also speculations that CIMP may generate inflammation-mediated OSCC. (Shaw et al., 2007)

In contrast to the scenario of chronic inflammation as incubating environment for cancer development, the immune system may also recognize cancerous cells as foreign and control tumor growth. In this context, two theories of "cancer immunosurveillance" and "cancer immunoediting" have recently been formed. Cancer immunosurveillance describes the total destruction of a developing tumor by the immune system. Increased incidence of tumors in immunosuppressed transplant patients has been described, whereas a strong immune reaction relates to favorable prognosis. The cancer immunoediting theory states that tumor development, because of its heterogeneity and diversity of distinct cell clones, can have different outcomes, either complete elimination or tumor formation. Inflammatory reactions have shown to promote tumor development and growth. (Bui and Schreiber, 2007) The controversy whether our immune system promotes or defends against cancer will persist. A probable explanation in this issue is the narrow definition of inflammation. It

would be reasonable to suggest a coexistence of these different inflammatory functions.

This project concentrates on three complementary approaches in modeling an inflammatory environment with squamous cell CpG methylation in the oral cavity. The role of inflammatory cells, oxidative and nitrosative stress, and interleukins is therefore explained in more detail.

1.3.1 Inflammatory Cells

Polymorphonuclear cells (PMNs), better known as neutrophils, and peripheral blood mononuclear cells (PBMCs), consisting of mainly lymphocytes and monocytes, are common inflammatory cells. PMNs are rather associated with acute inflammatory response, whereas PBMCs are frequently noticed in chronic inflammation. In the peripheral blood, PMNs circulate at a concentration of approximately 2 to 8 x 10^9/L with a life expectancy of only a few hours to days. Thus, the production of PMNs in the bone marrow and their release into the peripheral blood is a highly dynamic process. PBMCs have a blood concentration of approximately 1.5 to 5 x 10^9/L and a life expectancy of hours to weeks. Upon stimulation with phorbol myristate acetate (PMA) or phytohaemagglutinin (PHA), PMNs produce large amounts of reactive oxidative species (ROS) causing oxidative stress. (Campregher et al., 2008)

Campregher et al showed that PMA-activated PMNs can induce a G2/ M checkpoint arrest and replication errors in colon cancer cell lines. (Campregher et al., 2008) They further confirmed PMN-induced aberrant DNA hypermethylation by up-regulation of nuclear DNMT3a and 3b and stimulated DNMT1 and 3b mRNA expression. (Campregher et al., 2009)

1.3.2 Oxidative and Nitrosative Stress

ROS and reactive nitrogen species (RNS) generate oxidative and nitrosative stress, respectively, on the oral mucosa baring the capability to induce and

promote OSCC carcinogenesis. (Bagan and Scully, 2008) ROS and RNS play key roles in inflammation-driven carcinogenesis. During a normal inflammatory response, leukocytes produce high amounts of ROS and RNS to fight infections by inducing DNA damage in prokaryotes. However, ROS and RNS can also interact with the DNA of proliferating epithelial cells causing irreversible DNA modifications such as point mutations, deletions, single or double strand breaks. (Coussens and Werb, 2002)

Oxidative damage and stress are known to generate a higher incidence of mitochondrial mutations and to modify cellular proteins, mRNAs, as well as DNA. (Mithani et al., 2007; Campregher et al., 2008) ROS can produce 8-oxo-7,8-dihydro-2'-deoxyguanosine (8-oxodG), which is a source of DNA mispairing with adenine causing a C-to-A transversion but can be used as an indicator for oxidative DNA damage. RNS, like nitric oxide (NO), nitrogen dioxide (NO_2) and peroxynitrite ($ONOO^-$), are produced by inflammatory cells through expression of iNOS. Because of its oxidizing characteristics, RNS can damage an extensive range of molecules, including DNA and proteins within cells. Nitrosative stress in the form of NO can directly oxidize DNA, which typically results in mutagenic changes and damage of DNA repair proteins. (Balkwill and Mantovani, 2001) It has also been proposed that NO induces angiogenesis. (Sappayatosok et al., 2009) RNS can mediate the production of 8-nitroguanine, which can be used as indicator for nitrative DNA damage. (Chaiyarit et al., 2005)

1.3.3 Interleukin-6

Interleukins (ILs), components of the cytokine family, are cell-to-cell signaling molecules produced by a variety of immune and non-immune cells. IL-6 is one of the best-investigated cytokines and in the spotlight of numerous research projects, also in correlations with oral tumorigenesis. (Vairaktaris et al., 2008) The gene site encoding for IL-6 is located on chromosome 7p21. (Sassano et al., 2007) IL-6 is a multifunctional cytokine with pro- and anti-inflammatory

effects mediating the transition from innate to acquired immunity. (Ishihara and Hirano, 2002) IL-6 receptors can naturally be found in a membranous (IL-6R) or soluble (sIL-6R) form (Figure 4). The IL-6R is associated with the signal-transducing membrane protein gp130. This interaction of IL-6 on cells expressing gp130 through sIL-6R is called transsignaling. Natural inhibitor of transsignaling is the soluble receptor form sgp130. (Ishihara and Hirano, 2002; Jones et al., 2005) Upon activation and dimerization of gp130, the inner cellular signaling cascade is initiated and the associated Janus tyrosine kinases (JAKs) are activated. gp130 phosphorylation by JAKs activates the signal transducer and activator of transcription (STAT) 1 and STAT3. (Bromberg and Wang, 2009) It is known that active, phosphorylated STAT3 (pSTAT3) forms dimers, which can access the nucleus and activate specific genes involved in cell survival (bcl-2, bcl-x$_L$) and cell growth (cyclin D1). (Chakravarti et al., 2006) Through STAT3 activation, IL-6 induces tumor growth, proliferation and survival in various tumors. (Bromberg and Darnell, Jr., 2000; Chakravarti et al., 2006)
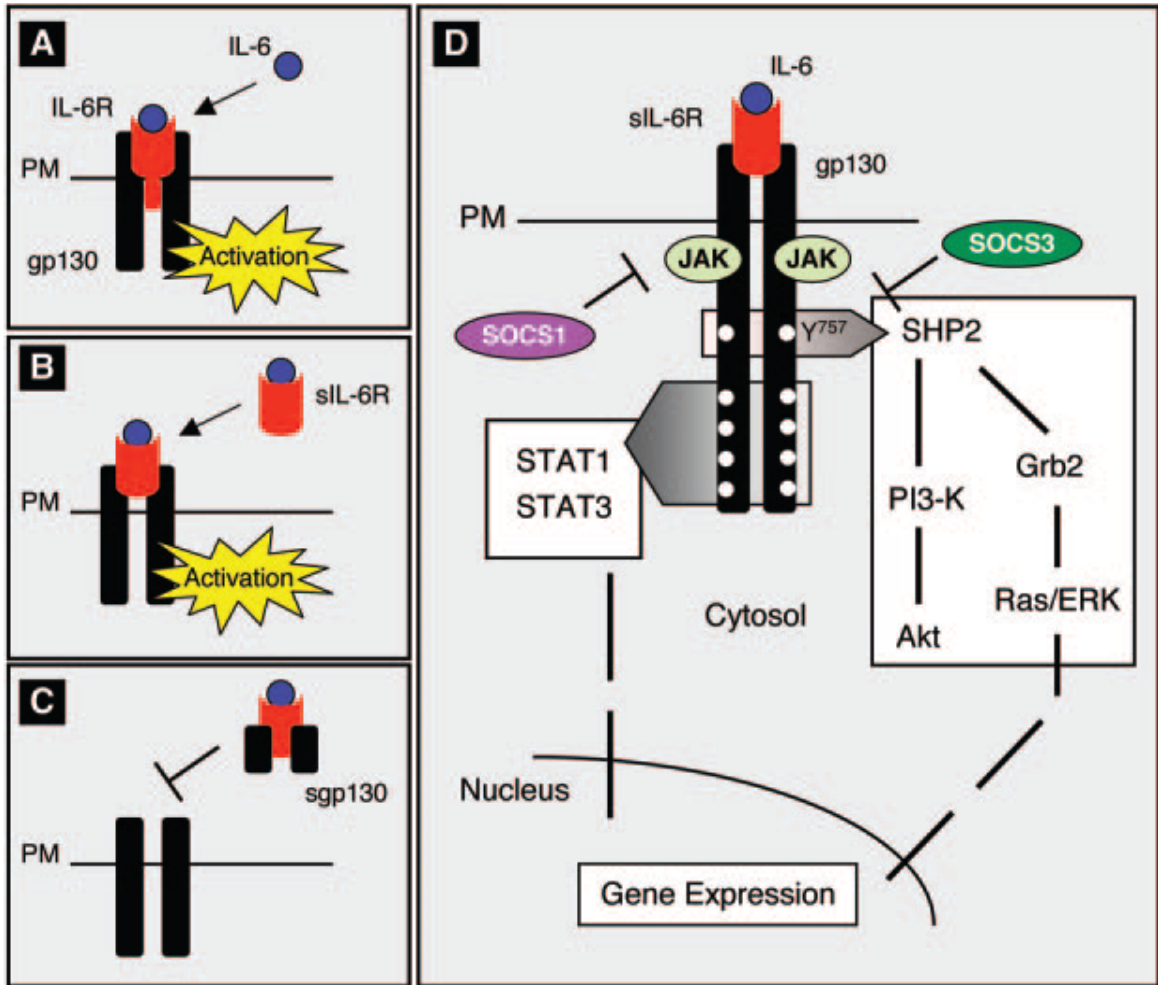
Figure 4 **IL-6 signaling cascade.** (Jones, 2005) A. Classic signal transduction with transmembranous IL-6 receptor (IL-6R) and gp130. B. Signal transduction through transsignaling with soluble IL-6 receptor (sIL-6R). C. Inhibition of transsignaling due to soluble gp130 (sgp130). D. Dimerization of gp130 activates Janus tyrosine kinases (JAKs) and subsequent phosphorylation of tyrosine residues (white circles), which further activate the signal transducer and activator of transcription (STAT) 1 and STAT3. Negative regulation is monitored by suppressor of cytokine signaling (SOCS) 1 and SOCS3.

IL-6 is partially responsible for the acute inflammatory response. (Ishihara and Hirano, 2002; Duffy et al., 2008) Persisting IL-6 concentrations mediate the transition from acute inflammation to chronic inflammation. IL-6 functions as T-

cell-regulator and polyclonal B-cell activator; thereby inducing the production of monoclonal antibodies. (Ishihara and Hirano, 2002; Jones, 2005) IL-6 supports the survival and growth of lymphocytes and myeloid cells. (Ishihara and Hirano, 2002) This interleukin plays a crucial part in chronic diseases regulating both local inflammatory events and related systemic symptoms such as the production of acute phase proteins (e.g. C-reactive protein). IL-6 has a major role in governing inflammation and is thought to be an excellent therapeutic target. (Jones et al., 2005)

While the cytokine level seems to be independent of the main risk factors such as tobacco and alcohol, chronic inflammation enhances the cytokine-based microenvironment significantly. (Rhodus et al., 2005) IL-6 is released by inflammatory cells, the neighboring mesenchymal tissue and by tumor cells themselves. (de Oliveira et al., 2009; Sassano et al., 2007) It seems to have regulating effects on cell survival, growth, proliferation, and differentiation of cancer cells and is associated with tumorigenesis, angiogenesis, and cachexia. (de Oliveira et al., 2009; Wang et al., 2002) IL-6 inhibits growth in various cells, whereas under pathological circumstances it appears to promote the growth of tumor cells. (Bromberg and Wang, 2009) IL-6 is believed to support tumorigenesis by tumor initiation and immune dysfunction. To further support the theory of IL-6's influence on oral tumorigenesis, OSCC cells were found to invade and metastasize into preferably IL-6-rich environment. (Duffy et al., 2008) IL-6, among other interleukins, activates the STAT3 cascade. High STAT3 levels have been mentioned in various tumors, linking IL-6 to tumorigenesis. (Chakravarti et al., 2006; Duffy et al., 2008; Calo et al., 2003; Bromberg and Darnell, Jr., 2000) One hypothesis states that IL-6 mediates STAT3-dependent tumorigenesis. Activated STAT3 is often found in the invasive front of tumor surrounding tissue. As STAT3 is responsible for the expression of important genes including bcl-x_L, survivin, and cyclin D, it contributes to their up-regulation in tumors. Injured intestinal epithelial cells not expressing STAT3 show an increased production of cytokines and a lower risk

of cancer. (Bromberg and Wang, 2009) In cancer, elevated serum IL-6 levels have been linked with immune unresponsiveness, cachexia, hypercalcemia, and wasting – all these factors are associated with poor prognosis. (St John et al., 2004)

As part of the immune response, IL-6, among other tumor-derived factors, recruits myeloid-derived suppressor cells (MDSC), which can be found in the peripheral circulation, lymphoid organs, and tumors of cancer patients. MDSCs act as immunosuppressors favoring tumor growth. In addition, they produce high quantities of ROS and an increased iNOS expression. These observations have led to the concept that chronic inflammation might act in an immunosuppressive manner thus promoting outgrowth of malignant cells. (Whiteside, 2009)

Studies have revealed increased IL-6 levels (highest compared to other interleukins) in saliva and serum of oral cancer patients. (Vairaktaris et al., 2008; Katakura et al., 2007; Sahebjamee et al., 2008) A significant increase in saliva IL-6 was measured in patients with oral lichen planus, suggesting that the enhanced presence of IL-6 in saliva is an early event of tumorigenesis. IL-6 has been proposed as promising diagnostic marker in saliva (high cytokine levels correlate with severity of dysplasia) and as prognostic marker for high recurrence and poor survival in serum. (Duffy et al., 2008; Sahebjamee et al., 2008; Rhodus et al., 2005) IL-6 is associated with bone invasiveness and radioresistance in HNSCC. (Chakravarti et al., 2006) Comparing OSCC with normal tissue, the expression of IL-6R and IL-6 mRNA transcripts is much higher in OSCC. Increased IL-6 mRNA correlates with a better prognosis, less distant metastasis, less lymph node involvement and less secondary primary tumors. (Wang et al., 2002)

1.4 Does Chronic Inflammation Alter DNA Methylation?

Chronic inflammation is a rather poorly-investigated risk factor of OSCC. It is yet unknown whether chronic oral inflammation influences aberrant DNA methylation, which could result in OSCC tumorigenesis.

The hypothesis of this project is that chronic inflammation of the oral cavity may specifically alter global DNA methylation and aberrant CpG island methylation, which might induce CIN, inactivate tumor suppressor genes, and consequently contribute to oral tumorigenesis.

We have therefore developed several in-vitro models to better understand the interaction of inflammatory blood cells, direct oxidative and nitrosative stress, and IL-6 on changes in methylation patterns in OSCC.

2 Materials and Methods

2.1 Cell Culture

Cell culture was performed at the cell line-specific conditions (Table 1): HaCaT, primary oral fibroblasts, CLS-354, Detroit 562, UM-SCC-14C and HCT116 were cultured in Iscove's Modified Dulbecco's Medium (IMDM, Invitrogen) supplemented with 10% fetal bovine serum (FBS). The cell lines SCC016, SCC056, SCC114 and SCC116 were cultured in Minimum Essential Medium-α (MEM-α, Invitrogen) supplemented with 10% FBS. Growth conditions were good at 37°C, 5%CO_2 and full humidity. For freezing purposes, the culture medium was supplemented with DMSO at 10%.

Table 1   Human cancer and non-cancer cell lines used in this project.

Cell Type	Human Cell Lines	Tissue Origin	Source
Non-cancer	HaCaT	immortalized keratinocytes (skin)	Baylor University Medical Center, Dallas, USA Division of Gastroenterology
	primary oral fibroblasts	gingiva	Texas A&M University, Dallas, USA Baylor College of Dentistry
OSCC	CLS-354 Detroit 562 UM-SCC-14C	tongue pharynx oral cavity	Medical University of Vienna, Austria Dept. of Head and Neck Surgery
	SCC016 SCC056 SCC114 SCC116	tongue tongue floor of mouth alveolar ridge	University of Illinois, Chicago, USA Dept. of Head and Neck Surgery
Control cancer	HCT116	colon	Baylor University Medical Center, Dallas, USA Division of Gastroenterology

2.2 Steady-State Methylation Status

Since we expected variations in the steady-state methylation status between certain cell lines, we analyzed the cells at the beginning to identify the most appropriate target cells for our experiments. The testing was performed with DNA of untreated cells using pyrosequencing (see chapter 2.6).

2.3 Inflammatory Cell Culture Models

2.3.1 Inflammatory Cells

We simulated an inflammatory environment in a co-culture model with the intent to measure its ability to induce aberrant DNA methylation. Non-cancer and selected OSCC cell lines were used as "targets". Both PMNs and PBMCs were attempted to be used as "effectors".

Blood sampling was approved by the Institutional Review Board of the Baylor Research Institute. Healthy volunteers gave informed written consent. 50mL whole blood (five 10mL BD Vacutainers containing Sodium Heparin) were captured from each individual. PMNs and PBMCs were isolated separately from fresh blood by Dextran (Fluka Analytical) sedimentation, Ficoll-Paque Plus (GE Healthcare) separation and centrifugation. PMNs settled down as a pellet, while PBMCs were collected from the cloudy, buffy ring. Afterwards, the cells were activated by 50ng/mL PMA (Sigma) as described. (Campregher et al., 2008) PMA activation induces hydrogen peroxide (H_2O_2) release in inflammatory cells. Superoxide release was verified by lucigenin (Sigma) treatment and measurement of its superoxide release with the Veritas Microplate Luminometer (Turner BioSystems, Sunnyvale, CA). Lucigenin oxidation is a common chemiluminescence reaction. Upon mixing of lucigenin with a solution containing superoxide, very bright green light is produced that decays to blue. Light is emitted by decay of the activated state to a lower energy level. This

change in color can be detected by the luminometer and correlates with the superoxide release of the PMA-activated inflammatory cells.

HaCaT, primary oral fibroblasts, Detroit 562 and SCC016 cell lines were seeded into 24-well-plates at a density of 20,000 cells/ well. The experiment was performed as a dose range study (different effector to target cell ratios at 100:1, 10:1, 1:1). Controls included non-activated PMNs (effector to target cell ratio at 100:1) and the addition of 200µM H_2O_2 as positive control. The co-culture system was set up in a 24-well-plate using a permeable membrane for separation of effector and target cells (Costar Transwell 0.4µm Polyester Membrane, Corning Inc.) to avoid cell contact but allow flow of soluble mediators. The inserts allow exchange of the inflammatory cells during multiple day co-culture. Due to the short life expectancy of the PMNs, the PMN isolation procedure was repeated daily from fresh blood, with the intention that every 24 hours fresh PMNs would induce inflammation thereby mimicking chronic inflammation. The culture medium was changed on a daily basis. Co-culture was performed for up to five days.

2.3.2 Oxidative and Nitrosative Stress

The second approach of inducing methylation in-vitro was the application of H_2O_2 and S-Nitroso-N-acetyl-DL-penicillamine (SNAP, Sigma) as donors of superoxide (O_2^-) and NO, respectively. HaCaT, primary oral fibroblasts, Detroit 562, UM-SCC-14C, SCC016 and SCC056 cell lines were seeded into 24-well plates at a density of 20,000 cells/ well. The experiment was carried out as dose range study with H_2O_2 concentrations of 200µM and 800µM and SNAP concentrations of 100µM, 300µM, and 500µM. The medium was changed every 24 hours. The experiments were performed for up to five days.

2.3.3 Interleukin-6

Also IL-6 (Sigma) was tested to induce methylation in the cell culture model. A western blot on STAT3/ pSTAT3 was initially performed to select the cell lines

that express IL-6R and phosphorylate STAT3. Such cells were selected for IL-6 experiments (see chapter 2.4.1). Also, IL-6 bioactivity was tested upon viability by an MTT assay (see chapter 2.5) to select appropriate treatment conditions.

HaCaT, SCC056, SCC114, SCC116, and HCT116 cell lines were treated with 100ng/mL IL-6. One set of treatment was performed for 24 hours. The second set of treatment was performed until confluence was reached after 72hours (SCC116) or 96hours (HaCaT, SCC065, SCC114, HCT116). To simplify further descriptions, we only distinguished between untreated (00h), 24h, and 96h IL-6 treatment.

DNA of HCT116 cells treated with 2.5µM 5-aza-2'deoxycytidine (5-AZA) for 24h and harvested after 48h of proliferation was added in some experiments as positive control. (Cheng et al., 2003)

2.4 Western Blot

Western blotting is a well-established method for protein expression analysis. The cell samples were denatured at 95°C for 10min, then loaded onto an SDS-polyacrylamid gel (containing Tris, acrylamide/ bis, SDS, TEMED, APS, and H_2O) and transferred onto a PVDF membrane (Amersham, GE Healthcare). The successful transfer of protein onto the membrane was reassured by Ponceau staining. The membranes were blocked with 5% non-fat milk in TBS-T for 30min. Blotting with the primary antibody was performed overnight at 4°C or for 2h at room temperature. The secondary antibody was added for 30min at room temperature. The proteins were visualized with ECL-Plus detection solution (Amersham, GE Healthcare) with the Storm 840 fluorescence imaging system (Amersham, GE Healthcare).

2.4.1 STAT3 and pSTAT3 Expression

To assure a proper IL-6 response, we tested its downstream activity for STAT3 phosphorylation. Binding of IL-6 to its receptor would activate the intracellular cascades causing an increase of pSTAT3. The cell lines HaCaT, primary oral fibroblasts, CLS-354, Detroit 562, UM-SCC-14C, SCC016, SCC056, SCC114, and SCC116 were tested for presence of IL-6R. HCT116 expresses IL-6R and functioned as positive control. (Zhang et al., 2007; Foran et al., 2009) The cell lines were treated with 10ng/mL IL-6 for 30min in cell culture. The cells were removed from the cell culture dish with 1x SDS buffer (containing 62.5mM Tris pH6.8, 10% glycerol, 2% SDS, 2mM EDTA, bromophenol blue, H_2O and freshly added 2% β-mercaptoethanol). Western blots were performed on a 10% SDS-polyacrylamid gel and blotted with STAT3 and pSTAT3 antibodies at a dilution of 1:500 (both by Santa Cruz).

2.4.2 DNMT1 and DNMT3b Expression

DNMT1 and DNMT3b protein expression was assessed in the 00h versus 96h IL-6-treated HaCaT, SCC056, SCC114, and SCC116 cells. The Western Blot was performed on a 7.5% SDS-polyacrylamid gel and blotted with DNMT1 (1:500; Santa Cruz) and DNMT3b (1:1,000; Cell Signaling) antibodies. Actin (1:10,000; Sigma) served as loading control.

As positive control, we performed a DNMT1 western blot with the colon cancer cell line HCT116 as described elsewhere. (Foran et al., 2009) Nuclear extraction utilizing the Universal Magnetic Co-IP kit (Active Motif) was performed on 00h, 24h and 96h IL-6-treated HCT116 cells. To the resulting supernatant of the extract, SDS-buffer and β-mercaptoethanol were added to reach an end concentration of 1x and 2%, respectively. With our standard protocol, the western blot was performed on a 7.5% SDS-polyacylamid gel and blotted with the DNMT1 (1:500; Santa Cruz) antibody. Actin (1:10,000; Sigma) served as general loading control. The proliferating cell nuclear antigen (PCNA, 1:500; Santa Cruz) served as nuclear loading control.

2.5 MTT Assay

3-(4,5-Dimethyl-2-thiazolyl)-2,5-diphenyl-2H-tetrazolium bromide, better known as MTT, was used for cell viability assays. The membrane-permeable yellow dye of MTT enters the cells. In living cells, mitochondrial reductases reduce MTT to form the dark blue product MTT-formazan (Figure 5). Measurement of MTT-formazan with spectrophotometry allows the quantitation of cell viability. In this context, MTT is used as a direct indicator for cytotoxicity and apoptosis.
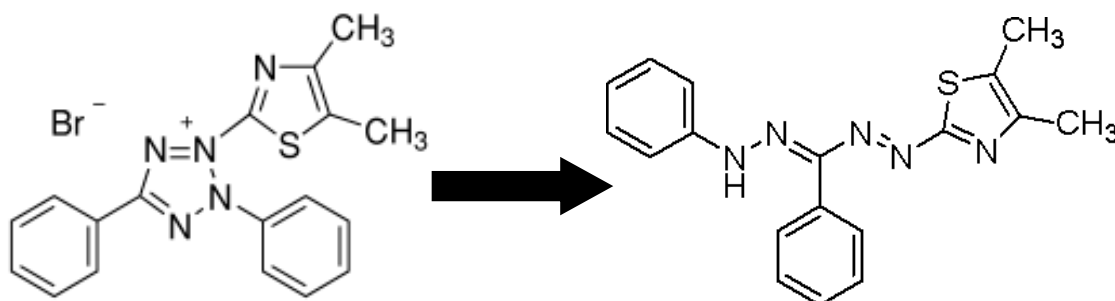

Figure 5   **Chemical structure of MTT (left) and its reduction to MTT-formazan (right).**

The cell lines HaCaT, SCC056, SCC114, and SCC116 were tested upon viability in the presence of IL-6. The IL-6 concentrations tested were 0, 5, 10, 20, 40, 80, and 160 ng/mL with a medium change every 24h. Cell viability was assessed at time points 0, 24, 48, 72, and 96h. After removing the medium, 100µL of MTT (0.5mg MTT/mL medium; Calbiochem and Sigma) were added to each well of the 96-well-plate, which was incubated at 37°C 5%CO_2 for 2-3h. 100 µL of lysis buffer (10% SDS in 0.01N HCl) were added to each well. The plate was covered with foil to keep off light and incubated at 37°C for 18-24h. The absorbance was measured colorimetrically at the single wavelength 570nm with a microplate reader (model 550, BioRad). The MTT assay was performed in triplicates.

2.6 Detection of the Methylation Status by Pyrosequencing

2.6.1 DNA Isolation and Bisulfite Modification

After harvesting cells from culture, DNA isolation was performed using the QIAamp DNA Mini kit (Qiagen). The DNA concentration was measured by spectrophotometry (DU530, Beckman Coulter). Bisulfite modification was performed with 300-500ng per sample with the EZ DNA Methylation Gold kit (Zymo Research). The bisulfite modification protocol was used with adjusted thermocycler setup (PTC-200 Peltier Thermal Cycler, MJ Research Inc.) for DNA denaturation: 95°C for 15min, 4°C for 30min, 75°C for 2h45min, 4°C forever. Bisulfite treatment converts only single-stranded unmethylated cytosine to uracil, while methylated cytosine does not react. (Ishida et al., 2005) Various methods take advantage of this bisulfite-induced sequence change and therefore detect 5-methyl-cytosines as these are the only cytosines left after successful bisulfite treatment. For more information on bisulfite treatment, the author refers elsewhere (Clark et al., 1994).

2.6.2 PCR and Gel Electrophoresis

The genes MGMT, RASSF2-1, SOCS1, SFRP2, APC1A, HPP1, P16, and LINE-1 were selected to perform pyrosequencing (Table 2).

Table 2   Tumor-associated genes of interest and their functions.

Gene	Full gene description	Function	Reference(s)
MGMT	O6-methylguanine DNA methyltransferase	DNA repair, detoxification, prevention of alkylation	(Esteller, 2002; Ha and Califano, 2006; Kato et al., 2006; Shaw, 2006)
RASSF 2-1	Ras association domain family 2-1	cell migration, cell cycle, colony formation	(Imai et al., 2008)
SOCS1	suppressor of cytokine signaling 1	negative feedback to cytokine signaling, postnatal IFN-gamma action	(Alexander et al., 1999)
SFRP2	secreted frizzled-related protein 2	Wnt signaling	(Sogabe et al., 2008)
APC1A	adenomatous polyposis coli 1A	Wnt signaling, prevention of cell overgrowth	(Uesugi et al., 2005)
HPP1	hyperplastic polyposis protein 1	unknown	(Shibata et al., 2002; Hamilton et al., 2006)
p16	cyclin-dependent kinase inhibitor 2A (CDKN2A)	cell cycle control	(Kato et al., 2006; Nakahara et al., 2006; Balkwill and Mantovani, 2001; Shaw, 2006)
LINE-1	long interspersed nucleotide element - 1	function unknown; used as surrogate marker for global DNA methylation	(Yang et al., 2004; Kim et al., 2009; Choi et al., 2009)

The bisulfite-modified DNA products were selectively amplified by polymerase chain reaction (PCR). For pyrosequencing, either the forward or reverse primer is tagged with biotin-labeling for further selection of one strand. The PCR reactions were performed in a mix containing HotStar Taq Polymerase (Qiagen), each primer (designed and ordered from IDT Integrated DNA Technologies, Table 3), the bisulfite-modified DNA and RNase-free water. MGMT, RASSF2-1, SOCS1, SFRP2, APC1A, HPP1, p16, and LINE-1 were selected as primers to amplify the sequence of interest. Depending on the primer's specifications and the cell line, the PCR conditions were accordingly adjusted for best specific primer binding to receive a clean PCR product. The PCR reaction contained approximately 12.5µL HotStar Taq (Qiagen), 1µL of each forward and reverse primer (10µM), 9.5µL water, and 2µL bisulfite-modified DNA to a final volume of 25µL. We used the PTC 200 Peltier Thermal Cycler (MJ Research Inc).

Table 3   Primers and assay design for PCR and pyrosequencing.

F- forward PCR primer; R- reverse PCR primer; SQ- pyrosequencing primer; StA- sequence to analyze; DO- dispensation order; *- biotinylated primer; Y- dispensation of C and T at CpG site; Tm- PCR annealing temperature

Gene		Primer Sequence (5' to 3')	Tm [°C]	cycles
MGMT	F	GGGATATGTTGGGATAGTT	51	50
	R*	CCCAAACACTCACCAAAT		
	SQ	GGATATGTTGGGATAGT		
	StA	TYGYGTTTTTAGAAYGTTTTGYGTTTYGAYGTTYGTAGGT TTTYGYGGTGYGTATYGTTTGYG		
	DO	ATCTGTCGTTAGTATCGTTAGTCTGTTCGTATCAGTCGC TATGTTCAGTCGCTAGTCGTGATCGTAGTC		
RASSF2-1	F	GTAGGGGTTGAAAAAGGTTA	55	45
	R*	AACTCAAATCCAACCAAACTA		
	SQ	GGGTTGAAAAAGGTTAA		
	StA	GGGGTTGGAGGGAGGGAGAGGAAGGAGGAGGGGAGY GAGGAGGGYGGGGYGTTYGGTTTTTAGTYGYGTGGTTA TYGTTTGTTTAGTTTGGTTGGATTTGA		
	DO	AGGTGAGAGAGAGAGAGAGGATGTCGAGATGTCGGTCA GTCGTTATGTCAGTCGTGTGATCGTG		
SOCS1	F	GTGGGTATTTTTTTGGTG	50	50
	R*	ACTACCATCCAAATAAAAAC		
	SQ	TGGGTATTTTTTTGGTG		
	StA	YGYGATAGTYGTTAGYGGAATTGTTTTTTYGT		
	DO	GTCTGTCGATATGTCGTATGTCGATAGTTCG		
SFRP2	F	GGGTTGGTTAAAGAGGAA	53	45
	R*	CTCCCTCTACCCCCTC		
	SQ	GTTAGGGTTTTGTAGTAT		
	StA	YGTGGGYGYGYGATTTYGAGGGGGGTAGAGGGAG		

	DO	GTCGTAGTCTGTCAGTCGTATTCGAG		
APC1A	F	GGAGAGAGAAGTAGTTGTGTAA	49	45
	R*	CTACACCAATACAACCACAT		
	SQ	AGAGAGAAGTAGTTGTGTAA		
	StA	TTYGTTGGATGYGGATTAGGGYGTTTTTTATTTTYGTYG GGAGTTYGTYGATTGGTTGGGTGTGGGYGTAYGTGATY GATATGTGGTTGTATTGGTGTAGTT		
	DO	GTCGTGATAGTCGATATGTCGTTGATTCAGTCGATGTCA GTCGATGTGTGTAGTCGTGATCGTGTATCGAT		
HPP1	F	GGGATTTTTATAGTATTATGATTA	52	45
	R*	AATTTAACTACTACTTCCCC		
	SQ	TTTTATAGTATTATGATTAG		
	StA	TTYGTGTAATTTTGTAGTAGTAAAYGGTTTTYGAGGAATA TAGGATYGYGGGGGGTYGGGTAGYGGGTTATTGAGTATT TYGYGGAYGGYGGTAGTAGAGGYGGYGGYGGTGGTAG TGGTATT		
	DO	ATCGTGTATTGTAGTAGTGATCTGTTCGAGATATAGTAT CAGTCGGTCGTATGTCGTATGAGTGATTCAGTCGTATCA GTCGTAGTAGATGTCAGTCTGTCGTG		
p16	F	AGGGGTTGGTTGGTTATTAG	59	50
	R*	CTACCTACTCTCCCCCTCTC		
	SQ	GGTTGGTTATTAGAGGGT		
	StA	GGGGYGGATYGYGTGYGTTYGGYGGTTGYGGAGAGGG GTAGAGTAGGTAG		
	DO	AGGTCGTATCAGTCGTAGTCTGTCAGTCGTAGTCGAG		
LINE-1	F	TTTTGAGTTAGGTGTGGGATATA	52	50
	R*	AAAATCAAAAAATTCCCTTTC		
	SQ	AGTTAGGTGTGGGATATAGT		
	StA	TTYGTGGTGYGTYGTTTTTTAAGTYGGTTTGAAAAGYG		
	DO	GTCGTGTAGTCTGTCGCTTATGTCGTGAATGTC		

The PCR products were separated on a 2% agarose gel and visualized by ethidium bromide staining and UV transillumination (Kodak Gel Logic 200 Imaging System) to confirm the sole presence of the requested amplified DNA sequence. The target should ideally be one clearly restricted band at the size of the expected product, except for little remaining primer below 100bp.

2.6.3 Pyrosequencing

The DNA methylation status was detected by pyrosequencing. (King and Scott-Horton, 2008) Pyrosequencing is a quantitative method, the "new generation" compared to methylation-specific PCR (MSP), accurately analyzing multiple CpG sites within one gene's promoter. (Shaw, 2006) This technique is a direct sequencing by synthesis method announcing the order of the incorporated nucleotides and detecting the percentage of methylation within the given sequence. (Yang et al., 2004)

The specific biotin-labeling of one of the DNA strands attaches to the streptavidin-coated sepharose beads. The DNA strands are separated by denaturation. With the Pyrosequencing Vacuum Prep Tool (Biotage), the unlabeled DNA strand is removed and only the bead-attached, biotin-labeled strands are left behind for sequencing. The single, purified DNA strands are then applied to a mixture with the specific pyrosequencing primer (Table 3) and annealing buffer.

These reactions are setup on a 96-well-plate and further processing is achieved by the PyroMark MD pyrosequencing machine (Biotage). Depending upon dispensation order (Table 3) of the assay design, the pyrosequencer adds each nucleotide one at a time. The nucleotide's incorporation at the 3'-end of the DNA strand emits ATP which in further reaction produces detectable light. In this project, the reverse primers are biotin-labeled leaving an anti-sense strand for the pyrosequencing. The nucleotides (PyroGold reagents, Biotage) are therefore added in sense. At CpG-sites, the sequencer is told to dispense both

nucleotides thymidine and cytidine. All originally methylated cytosine sites will bind cytidine, whereas the unmethylated cytosine sites have been converted to uracils and will therefore bind thymidine. To ensure complete bisulfite conversion, some designs include the dispensation of a cytidine in a non-CpG area expecting no residual cytidine signal. The percentage of methylation is calculated by the pyrosequencing software PyroMark MD v.1.0 (Biotage) for each CpG island analyzing the ratio of cytidine amount to the total cytidine and thymidine. The overall methylation status is the average of all measured CpG island methylation values of one analyzed gene. The pyrosequencing design and analysis is shown as example for LINE-1 in Figure 6.
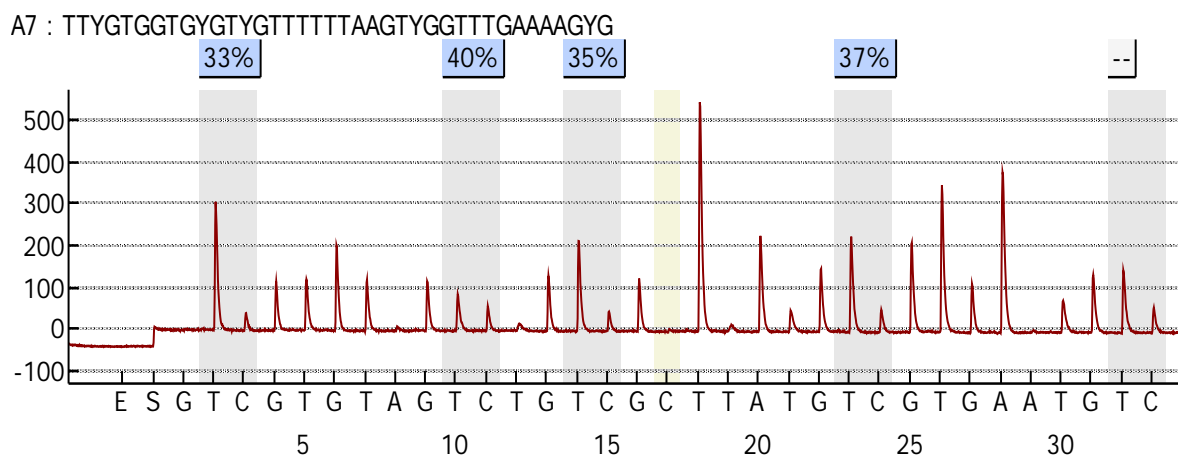
Figure 6 **LINE-1 pyrosequencing.** The graph shows the nucleotides in dispensation order, each peak standing for a specific nucleotide as labeled on the x-axis. The peak height represents the amount of the same nucleotide that is being incorporated to the DNA strand. The grey shaded areas mark the CpG sites: C-peaks stand for methylation, T-peaks stand for no methylation in this area. The boxes above the graph tell the methylation level at each CpG site.

2.7 Detection of the Methylation Status by MS-MLPA

The methylation-specific multiplex ligation-dependent probe amplification (MS-MLPA) is a semi-quantitative method distinguishing between unmethylated,

hemimethylated and methylated gene loci. The method won its recognition for straightforward investigation of the methylation status of multiple cancer-related genes in a single reaction. MS-MLPA works well with little amounts of DNA as low as 20ng and even with DNA extracted from paraffin-embedded tissue. No sodium bisulfite treatment is needed. We purchased the MS-MLPA kit ME002-A1 – Lot 1207, which is specific for a selected panel of tumor suppressor genes (MLPA, MRC Holland). This kit includes 27 Hha1-sensitive and 14 reference probes (Table 4).

Table 4   MS-MLPA probe panel of the ME002 kit. (MRC-Holland, 2009)

Length (nt)	SALSA MLPA probe	Hha1 site	Chromosomal position
64-70-76-82	Q-fragments: DNA quantity; only visible with less than 100 ng sample DNA		
88-92-96	D-fragments: Low signal of 88 or 96 nt fragment indicates incomplete denaturation		
136	Reference (CREM) probe 0981-L0566		10p12.1
142	**BRCA1** probe 3296-L1269	+	17q21
148	**BRCA2** probe 2285-L1776	+	13q12.3
154	Reference (PARK2) probe 3366-L2750		06q26
160	**ATM** probe 3023-L2413	+	11q23
166	**TP53** probe 2374-L2530	+	17p13.1
175	Reference (PTCH) probe 3708-L3162		09q22.3
184	**PTEN** probe 3808-L2169	+	10q23.3
193	**MGMT** probe 5670-L5146	+	10q26
202	Reference (MLH3) probe 1245-L0793		14q24.3
211	**PAX5** (PAX5a) probe 3750-L3210	+	09p13
220	**CDH13** probe 2257-L1742	+	16q24.2
229	Reference (PAH) probe 2334-L1820		12q23
238	**TP73** probe 1684-L1264	+	01p36
247	**WT1** probe 2755-L2204	+	11p13
256	Reference (PMP22) probe 1462-L0927		17p12
265	**VHL** probe 3818-L3850	+	03p25.3
274	**GSTP1** probe 2747-L2174	+	11q13
283	Reference (TSC2) probe 1832-L1397		16p13.3
292	**CHFR** probe 2737-L2164	+	12q24.33
301	**ESR1** probe 2746-L2173	+	06q25.1
310	Reference (TNXB) probe 3033-L2588		06p21.3
319	**RB1** probe 2734-L2161	+	13q14.2
328	**MSH6** probe 1250-L0798	+	02p16
337	Reference (APC) probe 1700-L1341		05q22
346	**THBS1** probe 1678-L1258	+	15q15
355	**IGSF4** probe 3816-L1179	+	11q23
364	Reference (PTEN) probe 3638-L2945		10q23.3
373	**STK11** probe 6783-L2167	+	19p13.3
382	**MGMT** probe 1681-L1261	+	10q26
391	Reference (PARK2) probe 2184-L1682		06q26
400	**PYCARD** (ASC) probe 2252-L1737	+	16p12
409	**PAX6** probe 3749-L3209	+	11p13
418	Reference (ATM) probe 2670-L2137		11q23
427	**CDKN2A** probe 1530-L3851	+	09p21
436	**GATA5** probe 3752-L3212	+	20q13.33
445	Reference (IL2) probe 0627-L0183		04q26
454	**RARB** probe 4046-L2172	+	03p24
463	**CD44** probe 4500-L2761	+	11p12
472	**RB1** probe 4502-L2199	+	13q14.2
481	Reference (CASR) probe 2683-L2148		03q21

The MS-MLPA probes consist each of two olgionucleotides (Figure 7). The short synthetic olgionucleotide consists of the forward primer region and half of the target-specific region. The long M13-derived olgionucleotide consists of the other half of the target-specific sequence, a suffer sequence in probe-specific

lengths, and the reverse primer. The target-specific region is necessary for hybridization with the specific gene loci of the sample DNA, for ligation of the two olgionucleotides and it contains the CGCG-recognition sequence for the methylation-sensitive endonuclease Hha1. Thus, methylated sites are spared by Hha1, so that only the ligase will act upon its nucleotides and assemble the two olgionucleotides into one replicable sequence. The stuffer sequence with its probe-specific lengths is needed for fragment differentiation during sequencing.
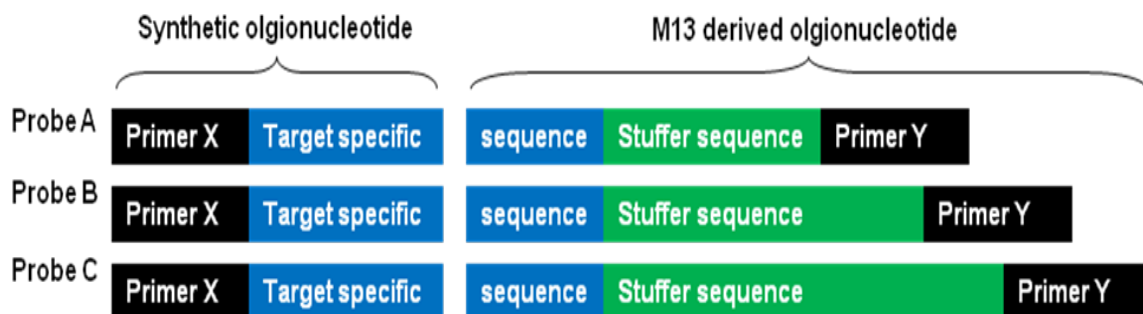
Figure 7 **MLPA probe design.** Modified from (Nygren et al., 2008) The MLPA probes are each made of two olgionucleotides. Together, they consist of forward (X) and reverse (Y) primer, a target-specific sequence for hybridization with the sample DNA, which includes the Hha1 recognition site and the ligation site, and a stuffer sequence with probe-specific length for fragment differentiation during sequencing.

The MS-MLPA protocol starts with denaturation of the sample DNA into single DNA strands and hybridization with the target-specific sequence of the two corresponding olgionucleotides (Figure 8). The samples were overlaid with mineral oil during this 60°C overnight incubation step to prevent high variations of salt concentration due to evaporation. After hybridization, each sample is split into two: one is treated with ligase only (ligation reaction aka "uncut" sample) and the other is treated with the methylation-sensitive endonuclease HhaI and ligase (digestion reaction aka "cut" sample). Ligation is the key step to successful PCR. For exponential fragment replication, PCR is performed with a FAM*-labeled forward primer with the sequence *GGGTTCCCTAAGGGTTGGA

and a reverse primer with the sequence GTGCCAGCAAGATCCAATCTAGA. The fragments attached to the blue dye FAM can then be identified by the sequencing machine ABI Prism 3100 Avant Genetic Analyzer (Applied Biosystems). The data was collected by the Data Collection Software Version 2.0 (Applied Biosystems), basic fragment analysis was performed by the Gene Mapper Software Version 3.5 (Applied Biosystems) and specific MS-MLPA analysis was completed with the Coffalyser Software (MLPA, MRC Holland). The methylation status is detected by comparing the peaks of the corresponding digestion and ligation reaction.
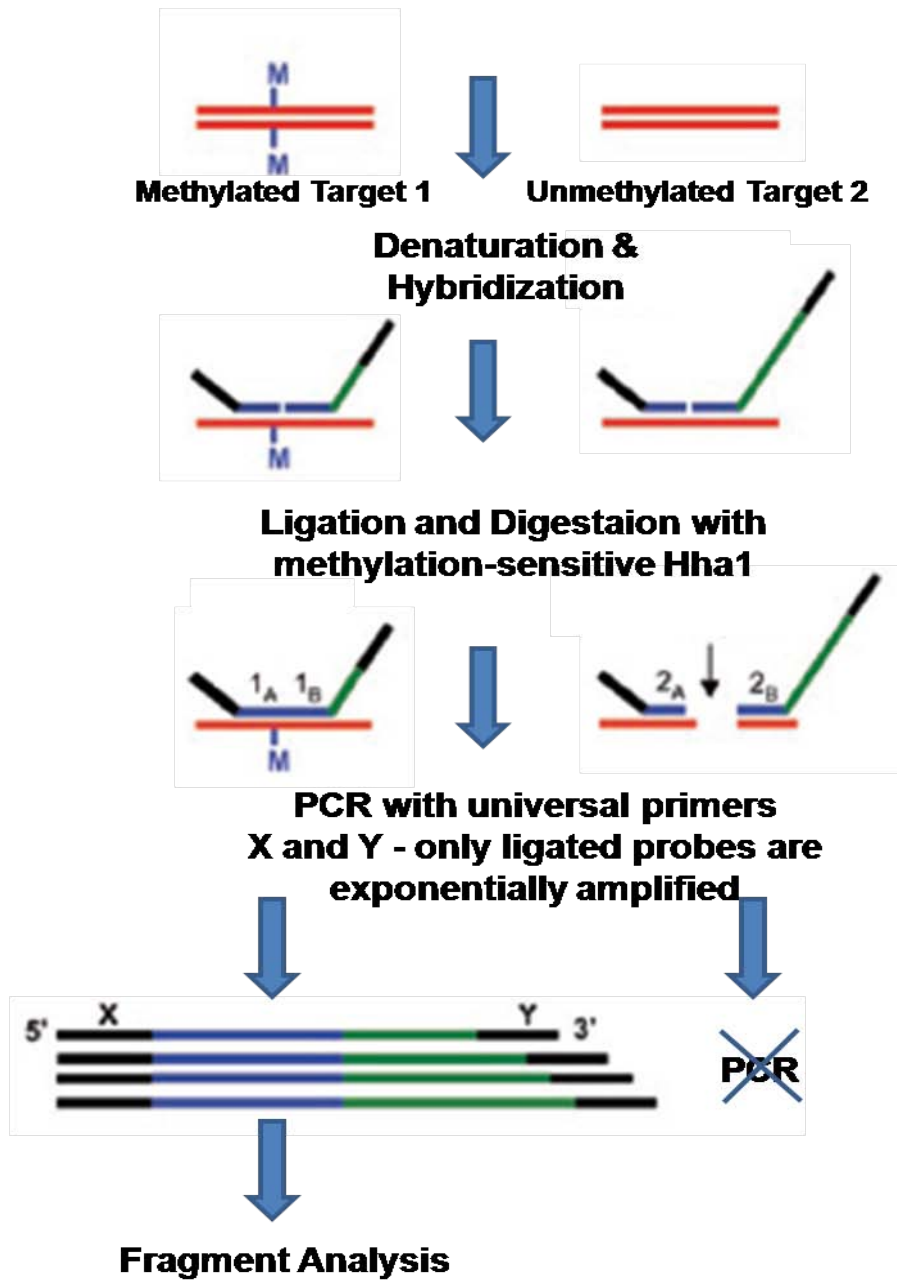
Figure 8   **Simplified concept of methylation-specific multiplex ligation-dependent probe amplification (MS-MLPA).** Modified from (Nygren et al., 2008). The figure shows the digestion reaction comparing the results of unmethylated versus methylated CpG sites. After denaturation of the DNA strands, the target-specific sequence of both olgionucleotides hybridizes to the DNA strand. In the digestion reaction, in case of methylated DNA, the probe is ligated, while unmethylated DNA attracts the methylation-sensitive

restriction enzyme Hha1 resulting in digestion. Only intact probes are further amplified by PCR and detected during sequencing.

To assure quality control, the MS-MLPA kit includes Q-fragments (64, 70, 76, 82nt) as verification of sufficient DNA amount and D-fragments to assure successful ligation, denaturation (88nt, 96nt),and hybridization (92nt). In any DNA reaction, the Q-fragments should be represented by very low peaks, while the D-fragments should show high peaks. In a blank (no DNA) reaction, however, the Q-fragments should be high, while the D-fragments and any of the probe signals should not be present.

DNA extraction is performed prior to MS-MLPA with the QIAamp DNA Mini kit (Qiagen). The DNA concentration is measured by spectrophotometry (DU530, Beckman Coulter). In this project, MS-MLPA was performed on 100-200ng of DNA from the cell lines SCC056, SCC114, SCC116, HaCaT, and HCT116. The experiment was performed for 00h, 24h, and 96h of treatment with 100ng/mL IL-6.

The PTC 200 Peltier Thermal Cycler (MJ Research Inc) was used to perform the denaturation/ hybridization, ligation/ digestion and PCR reaction. MS-MLPA was performed as recommended in its protocol with a few modifications: The denaturation was performed for 30min, mineral oil was added to prevent evaporation in the denaturation/ hybridization step, and the PCR protocol was adjusted to reduce non-specific probe peaks. The PCR reaction contained 2µL SALSA PCR Buffer, 20.5µL H_2O, 2.5µL ligation or digestion reaction, and 5µL Polymerase Mix. The annealing step of the PCR reaction was modified to 62°C for 30s. The MS-MLPA procedure was performed under the same conditions for all samples to assure precision allowing direct comparison of the analysis. Fragment analysis was performed on sequencing reactions each containing approximately 9µL Hi-Di Formamide (Applied Biosystems), 0.3µL Gene Scan ROX-500 size standard (Applied Biosystems), and 0.5µL of each PCR product. If necessary, the DNA amount was then accordingly adjusted. The reactions

were denatured at 89°C for 2min, chilled on ice, and loaded onto the ABI Prism 3100 Avant Genetic Analyzer sequencing machine (Applied Biosystems).

2.8 Detection of the Methylation Status by SMART–MSP

Due to the drawbacks of the commonly used method MSP, the method of Sensitive Melting Analysis after Real Time – Methylation Specific PCR (SMART-MSP) was established. SMART-MSP is a quantitative method which can identify false-positives due to an aberrant melting curve.

This method utilizes real time PCR (qPCR) followed by a dissociation analysis. For purpose of normalizing to the input DNA, COL2A1 has been introduced as an adequate control assay. The COL2A1 control assay primers have been designed to be totally independent of the CpG island methylation status. The COL2A1 primers were selected in a way that the amplified sequence would not include any CpG islands. Therefore, SMART-MSP allows for quantitative analysis of the methylation status. Accurate data can be obtained in the range of 100% to 0.1% methylation. (Kristensen et al., 2008)

To obtain quantitative data, normalization to 100% is necessary. Applying a standard protocol, DNA of the human lymphoma cell line raji was treated with the methyltransferase SssI methylase (New England Biolabs) and purified to obtain 100% methylated DNA, which was included as additional sample during SMART-MSP.

SYBR Green attaches to double-stranded DNA. The SYBR Green dye binds to every new copy of double-stranded PCR amplicon. During qPCR, the DNA-dye-complex absorbs blue light (λmax= 488nm) and emits green light (λmax= 522nm). The amount of green light emitted correlates with the amount of double-stranded DNA, which is measured after each cycle. The increase in fluorescence intensity is proportionate to the amount of PCR amplicons

produced during each cycle. With this method, the amount of PCR product is quantified.

During the dissociation protocol, the temperature is slowly increased separating double-stranded into single-stranded DNA. This phenomenon, called melting, occurs at a temperature specific for each sequence and shows a different melting profile (left or right shift) in case of heterogeneous methylation, false priming or incomplete bisulfite conversion. Thus, false-positive results, non-specific products, primer dimers or low background methylation can be identified due to different melting profiles. In this way, samples, which would show false-positive results during MSP, can be excluded from analysis.

The qPCR reaction contained 12.5µL SYBR Green (Applied Biosystems), 0.5µL of each forward and reverse primer solution (10µM, IDT Integrated DNA Technologies), 9.5µL water, and 2µL bisulfite-modified DNA from previous pyrosequencing experiments to a final volume of 25µL (Table 5). The primers were designed to attach to methylated sequences only. The qPCR protocol was launched with one cycle of 50°C for 2min and 95°C for 10min, followed by 45 cycles of 95°C for 20s, the gene specific annealing temperature (Tm) for 30s and 72°C for 30s. The dissociation protocol started at 60°C. We used the ABI Prism 7000 Sequence Detection System (Applied Biosystems) and the samples were run in duplicates. Calculation of the methylation status with normalization was performed applying a relative $2^{(-\Delta\Delta Ct)}$ quantification.

Table 5   **SMART-MSP primers.**

M- primer for methylated sequence; U- primer for unmethylated sequence; F- forward primer; R- reverse primer; Tm- qPCR annealing temperature

Gene	M/U	F/R	Primer Sequence (5' to 3')	Size [bp]	Tm [˚C]
COL2A1	M	F	GTAATGTTAGGAGTATTTTGTGGGTA	86	60
		R	CTACCCCAAAAAAACCCAATCCTA		
CHFR	M	F	GGATTAAAGATGGTCGAGC	101	56
		R	GATTAACTAACGACGACGCT		
GATA5	M	F	AGTTGTATTGGTTCGGGTTTC	101	60
		R	GACCGTAAAACCACGTAACC		
PAX6	M	F	GGAGTATTTAATCGGTTGGC	136	56
		R	AATAAAACCGAACCACGATT		

The cycle threshold value (c_T) is the number of cycles that have to be performed until an apparent amount of PCR products has been generated during the early exponential phase of the reaction. In other words, the cycle threshold value is different for each sample and tells how many cycles were needed, each doubling the PCR amount, to reach the same amount of PCR amplicons. Less methylation will result in less PCR product and therefore a high c_T-value. The c_T-value is obtained for each sample and used for analysis.

2.9 RNA Expression by qRT-PCR

Quantitative reverse-transcriptase polymerase chain reaction (qRT-PCR) is a method commonly used for RNA expression analysis. RNA is present for all expressed proteins. By converting the RNA into complementary DNA (cDNA) by reverse transcriptase, the cDNA can then be quantitatively measured by qPCR, which correlates to the amount of RNA expressed.

Total RNA isolation was performed with the RNeasy Plus kit (Qiagen) and stored at -80°C. RNA concentration was measured by spectrophotometry (DU530, Beckman Coulter). cDNA was prepared of 1µg RNA using the Advantage RT-for-PCR kit (Clontech) and stored at -20°C. The qRT-PCR reaction contained 12.5µL SYBR Green (Applied Biosystems), 0.5µL of each forward and reverse primer solution (10µM, IDT Integrated DNA Technologies), 9.5µL water, and 2µL cDNA to a final volume of 25µL (Table 6). The qRT-PCR protocol was launched with one cycle of 50°C for 2min and 95°C for 10min, followed by 45 cycles of 95°C for 15s and 60°C for 1min. The dissociation protocol started at 60°C. We used the ABI Prism 7000 Sequence Detection System (Applied Biosystems) and the samples were run in duplicates. Calculation of the gene expression with normalization was performed applying a relative $2^{(-\Delta\Delta Ct)}$ quantification. qRT-PCR was also setup for β-actin, which was utilized as normalization control.

Table 6 **qRT-PCR primers.**

F- forward primer; R- reverse primer; Tm- qPCR annealing temperature

Gene	F/R	Primer Sequence (5' to 3')	Size [bp]	Tm [˚C]
β-actin	F	GCCCTGAGGCACTCTTCCA	100	60
	R	CGGATGTCCACGTCACACTTC		
CHFR	F	CAGGATCAGGAGGATTTGGA	157	60
	R	CCTCCATCTTGTCTGGCTTC		
GATA5	F	CACCTTCGTGTCCGACTTCT	123	60
	R	CAGGCATTGCACAGGTAGTG		
PAX6	F	CCGGCAGAAGATTGTAGAGC	119	60
	R	CGTTGGACACGTTTTGATTG		

2.10 Statistical Analysis

2.10.1 Pyrosequencing

Pyrosequencing evaluates the average methylation of all CpG sites included in the assay. A change in methylation is significant if it causes a change in gene expression, which occurs at gene-specific levels. Consequently, there is no calculation to detect the significance of a methylation change. However, it is possible to determine whether a change in methylation occurred due to treatment or just by accident. This statistical test for significance was performed using a repeated measures-ANOVA test to compare methylation percentages at 00h versus 24h versus 96h of IL-6 treatment. A p-value of $p < 0.05$ was considered significant.

2.10.2 MS-MLPA

The MS-MLPA analysis was performed with the Coffalyser software (MLPA, MRC Holland). For analysis of the methylation status, the "uncut" samples were set as reference runs and the "cut" sample as sample runs. The analysis was performed with the "methylation status analysis" for each cell line separately. The software performed normalization and corrected for sloping. To look for a change in methylation due to induced inflammation by IL-6, the ratios of the untreated sample were compared to the ratios of the 24h and 96h IL-6-treated samples. MS-MLPA is a semi-quantitative method. Methylation changes were distinguished according to color.

Statistical analysis was performed to test the reproducibility of the MS-MLPA results with a Spearman's rank correlation test. For this calculation, exact MS-MLPA ratios were used and ratios above 1 were considered as 1.

2.10.3   SMART-MSP

SMART-MSP is a quantitative method. To analyze the SMART-MSP data, a relative $2^{(-\Delta\Delta CT)}$ quantification was chosen to normalize for different initial DNA amounts by adding the COL2A1 control assay, which is totally independent of CpG islands. The SssI-treated sample is considered as 100% methylated and added for further normalization.

For each sample, the c_T-value of each target gene is subtracted from its corresponding COL2A1 c_T -value, which results in the $-\Delta c_T$ value. For each genes, this $-\Delta c_T$ value of the 100% methylated sample is then subtracted from the $-\Delta c_T$ of each individual sample, resulting in the $-\Delta\Delta c_T$ value. Using the formula $2^{(-\Delta\Delta CT)}*100$ results in the methylation percentage of each sample in relation to the 100% methylated control.

2.10.4   qRT-PCR

qRT-PCR is a quantitative method used to investigate the gene expression. To analyze the qRT-PCR data, a relative $2^{(-\Delta\Delta CT)}$ quantification was chosen to normalize for different initial cDNA amounts by adding the β-actin control assay. For further normalization, the gene expression is normalized to untreated cells assuming an expression level of 100%. The $2^{(-\Delta\Delta CT)}$ calculations are performed as in chapter 2.10.3 and results represent the percentage of gene expression.

3 Results

3.1 Steady-State Methylation Status

For our experiments, several OSCC cell lines from different oral origins were included. Further, we chose the immortalized skin keratinocytes cell line HaCaT and primary oral fibroblasts to simulate rather "normal" cell states. The colon cancer cell line HCT116 functioned as control. The steady-state methylation level of these target cell lines was evaluated by pyrosequencing (Table 7).

Table 7   **Steady-state methylation status of target cells.**
n.a.- data not available

Cell Lines	MGMT [%]	RASSF 2-1 [%]	SOCS 1 [%]	SFRP2 [%]	APC1A [%]	HPP1 [%]	p16 [%]
CLS-354	76	6	n.a.	43	n.a.	77	2
Detroit 562	1	10	43	73	1	45	n.a.
UM-SCC-14C	1	8	27	95	2	81	1
SCC016	1	11	3	3	93	78	96
SCC056	1	2	85	79	2	81	n.a.
SCC114	1	8	7	2	94	79	96
SCC116	1	11	5	3	94	71	96
HaCaT	3	2	8	35	2	5	14
fibroblasts	2	2	5	1	2	3	2

Based on the steady-state methylation status, cell lines and genes were accordingly chosen for further experiments. In order to induce further CpG hypermethylation, high methylation levels would be inadequate for further experiments. p16 was dropped because it was difficult to amplify in two cell lines and showed high CpG methylation in the SCC cell lines. The cell line CLS-354 was excluded from the panel due to high methylation levels and difficult PCR amplification in two genes.

Primary human fibroblasts served as negative control and did not show a relevant amount of methylation at any of the sites. HaCaT, a pseudo-normal immortalized cell line, showed low methylation with the exception of SFRP2. All tumor cell lines displayed high steady-state CpG methylation levels above 50% in at least two of the investigated genes. The difference in methylation status between HaCaT and primary oral fibroblasts on one hand and the oral tumor cell lines on the other hand already points to the importance of CpG hypermethylation during tumor development.

3.2 PMN Co-Culture

PMNs and PBMCs were used to stimulate an inflammatory environment in a co-culture model. Activation with PMA increases the release of superoxide. The ROS release was measured in untreated cells and PMA-treated cells (Figure 9).
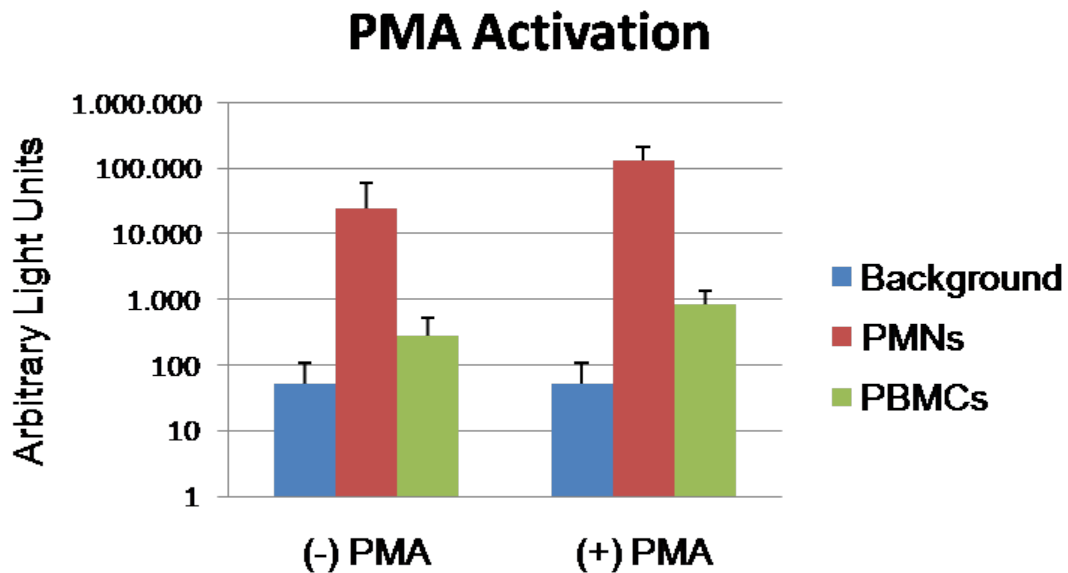
Figure 9   Activation of polymorphonuclear cells (PMNs) and peripheral blood mononuclear cells (PBMCs). Lucigenin-amplified chemiluminescence activates superoxide release by PMNs and PBMCs. After extraction from whole blood, cells were activated

with 50ng/mL Phorbol 12-myristate 13-acetate (PMA) for 30min. The graph shows the reactive oxygen species (ROS) release of $1x10^6$ PMNs or PBMCs directly after performed activation. Lucigenin without cells serves as negative control in the luminometer. The data points represent the mean of nine measurements for lucigenin only (background), four measurements for PBMCs and five measurements for PMNs. Standard deviations are shown as bars.

In our experiments, PMA activation increased the ROS release by a factor of 3 in PBMCs (average increase from 280 to 860) and by a factor of 5 in PMNs (average increase from 25,000 to 134,000). The strong increase in ROS release in activated PMNs suggests that these cells might be an excellent source to produce an inflammatory environment. Due to the higher absolute amount and the better activation, PMNs were selected for further experiments. Due to inefficient activation, PBMCs were inadequate and excluded from our experiments.

Co-culture was performed for five days at different effector-to-target cell ratios (100:1, 10:1, 1:1). 200µM H_2O_2 served as positive control for oxidative stress, while non-activated PMNs at ratio 100:1 were used as negative control (although they also produce a lot of ROS). DNA from treated target cells underwent pyrosequencing to detect possible changes in methylation pattern (Table 8).

Table 8 **Methylation status after 5 days of PMA-activated PMN treatment.**

na PMNs- non-activated PMNs; n.a.- data not available; *- data from steady-state methylation experiment (Table 7)

Cell Lines	Treatment	MGMT [%]	RASSF 2-1 [%]	SOCS 1 [%]	SFRP2 [%]	APC1A [%]	HPP1 [%]
Detroit 562	untreated*	1	10	43	73	1	45
	H_2O_2 200µM	1	13	n.a.	73	n.a.	n.a.
	PMNs 100:1	1	8	n.a.	66	1	50
	PMNs 10:1	1	10	43	71	2	52
	PMNs 1:1	1	14	42	68	2	47
	na PMNs	1	12	42	65	2	47
SCC016	untreated*	1	11	3	3	93	78
	H_2O_2 200µM	1	n.a.	1	9	93	82
	PMNs 100:1	1	9	5	2	92	83
	PMNs 10:1	1	10	4	1	92	83
	PMNs 1:1	1	10	3	2	92	83
	na PMNs	1	10	2	3	93	82
HaCaT	untreated*	3	2	8	35	2	5
	H_2O_2 200µM	2	3	2	33	2	5
	PMNs 100:1	2	3	2	30	2	4
	PMNs 10:1	2	3	2	32	2	4
	PMNs 1:1	2	3	3	31	2	4
	na PMNs	2	3	2	31	2	4
fibroblasts	untreated*	2	2	5	1	2	3
	H_2O_2 200µM	n.a.	1	n.a.	5	n.a.	n.a.
	PMNs 100:1	2	1	2	1	2	3
	PMNs 10:1	2	1	4	1	2	4
	PMNs 1:1	2	2	2	1	1	2
	na PMNs	2	1	1	1	2	3

Upon co-culture with PMA-activated PMNs, no change in methylation status was observed in any of the cell lines investigated except for minor deviations. We conclude that PMN treatment was unable to induce a change in methylation within these selected genes and cell lines. Even the positive control H_2O_2, as a direct source of ROS, was unable of inducing aberrant CpG methylation levels.

3.3 H_2O_2 and SNAP Treatment

As the second inflammatory approach, direct oxidative and nitrosative stress were applied in-vitro (Table 9). H_2O_2 as donor of superoxide and SNAP as donor of nitric oxide were added to the cell culture for five days. The experiment was carried out as a dose range study with H_2O_2 concentrations of 200µM and 800µM and SNAP concentrations of 100µM, 300µM, and 500µM with a medium change every 24h.

Table 9   Methylation status after 5 days of H_2O_2 and SNAP treatment.

n.a.- data not available; *- data from steady-state methylation experiment (Table 7)

Cell Lines	Treatment	MGMT [%]	SOCS1 [%]	SFRP2 [%]
Detroit 562	untreated*	1	43	73
	H_2O_2 200µM	1	n.a.	n.a.
	H_2O_2 800µM	n.a.	n.a.	98
	SNAP 100µM	2	n.a.	n.a.
	SNAP 300µM	n.a.	n.a.	78
	SNAP 500µM	n.a.	n.a.	n.a.
UM-SCC-14C	untreated*	1	27	95
	H_2O_2 200µM	n.a.	n.a.	78
	H_2O_2 800µM	n.a.	n.a.	96
	SNAP 100µM	1	23	94
	SNAP 300µM	n.a.	20	92
	SNAP 500µM	1	n.a.	96
SCC016	untreated*	1	3	3
	H_2O_2 200µM	n.a.	n.a.	n.a.
	H_2O_2 800µM	n.a.	n.a.	n.a.
	SNAP 100µM	1	n.a.	5
	SNAP 300µM	1	n.a.	1
	SNAP 500µM	2	n.a.	4
SCC056	untreated*	1	85	79
	H_2O_2 200µM	n.a.	n.a.	98
	H_2O_2 800µM	n.a.	n.a.	n.a.
	SNAP 100µM	1	n.a.	n.a.
	SNAP 300µM	13	n.a.	79
	SNAP 500µM	n.a.	n.a.	82
HaCaT	untreated*	3	8	35
	H_2O_2 200µM	1	4	31
	H_2O_2 800µM	1	n.a.	n.a.

	SNAP 100µM	2	n.a.	30
	SNAP 300µM	2	5	28
	SNAP 500µM	2	4	30
fibroblasts	untreated*	2	5	1
	H_2O_2 200µM	4	n.a.	1
	H_2O_2 800µM	n.a.	n.a.	n.a.
	SNAP 100µM	2	6	2
	SNAP 300µM	1	n.a.	1
	SNAP 500µM	n.a.	n.a.	n.a.

Although H_2O_2 and SNAP appear to be an adequate source of ROS and NOS by directly donating superoxide and nitric oxide, respectively, both agents were unable to induce methylation changes within five days of repeated treatment within the selected genes and cell lines.

3.4 IL-6 Treatment

3.4.1 STAT3 and pSTAT3 Expression

IL-6 treatment can only affect cells expressing the IL-6 receptor complex (IL-6R and gp130). To select appropriate cell lines for further experiments using IL-6 as proinflammatory stimulus, western blots were performed testing for phosphorylation of STAT3 upon treatment with IL-6 (Figure 10). HCT116 colon cancer cells served as positive control. (Foran et al., 2009) Cells expressing IL-6R are expected to show an increase in pSTAT3 as a consequence to IL-6 treatment.
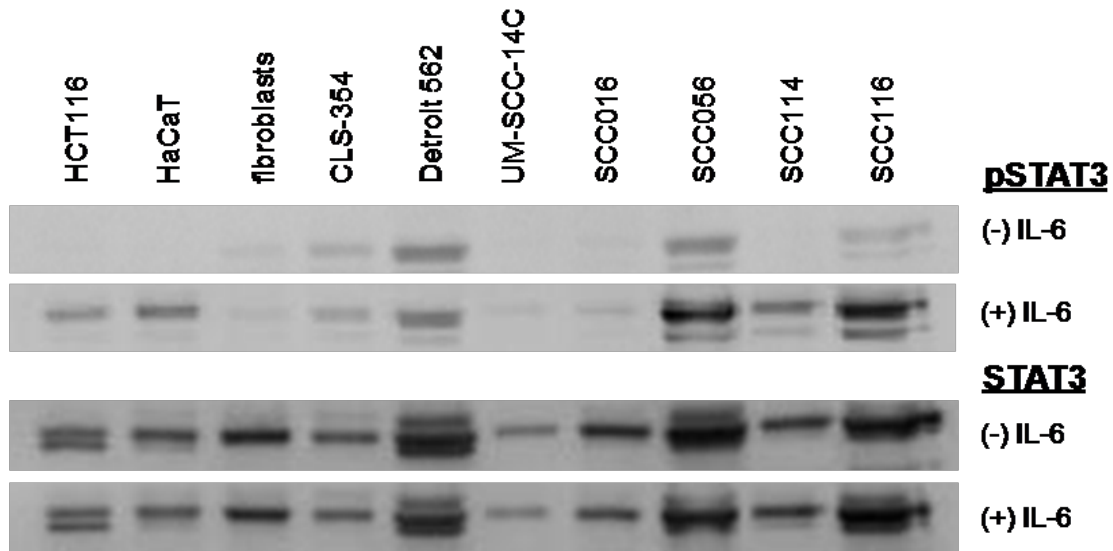
Figure 10 **Western Blot for pSTAT3 (91/86kDa) and STAT3 (91/86kDa)
expression in IL-6 treated (+) and untreated (-) cell lines.** The
cell lines HCT116, HaCaT, SCC056, SCC114 and SCC116 clearly
show STAT3 phosphorylation upon IL-6 treatment. The STAT3
blot was performed as loading control and shows equal loading
comparing the same samples with and without IL-6 treatment, but
different amounts comparing different cell lines.

An apparent increase in pSTAT3 expression between IL-6-treated and
untreated cell lines can be noticed in HCT116, HaCaT, SCC056, SCC114, and
SCC116 suggesting the presence of a functional IL-6 signaling cascade.
Therefore, these cell lines were chosen for further IL-6 experiments.

3.4.2 MTT Assay Results

The viability of the selected cell lines HaCaT, SCC056, SCC114, and SCC116
in the presence of IL-6 was crucial to further experiments and therefore
assessed by an MTT assay (Figure 11). Treatment was performed for up to 96
hours. IL-6 concentrations ranged from 5 to 160ng/mL. The average value of
the colorimetrical measurements of each triplicate was calculated and
normalized to the negative PBS control (100% viability assumed) for each day.

SCC056
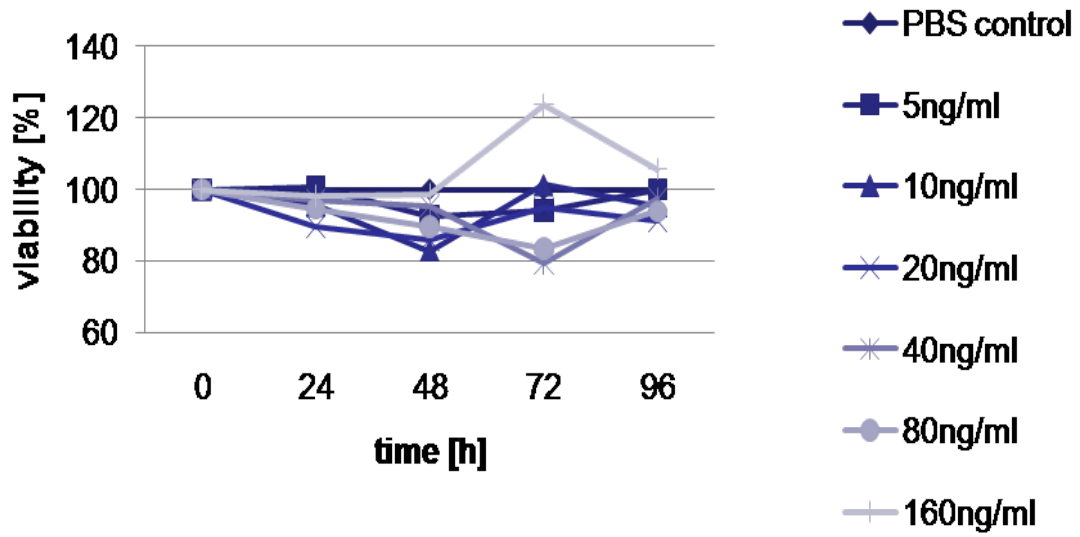
SCC114
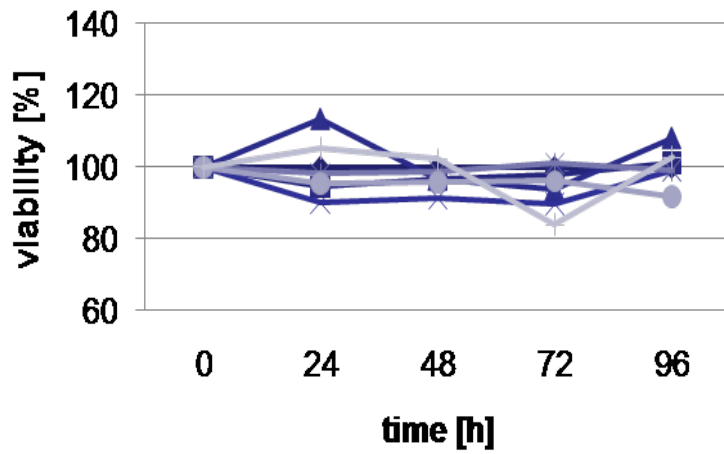
SCC116
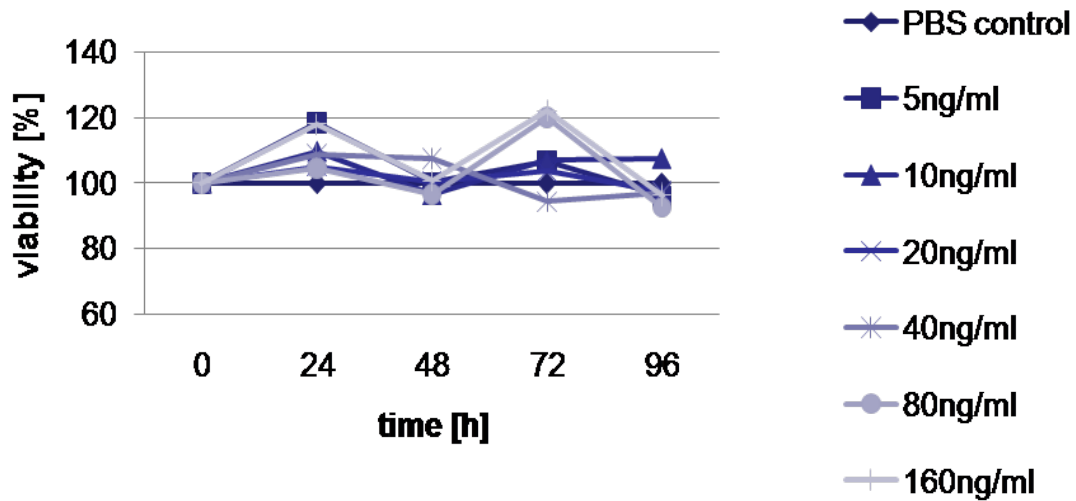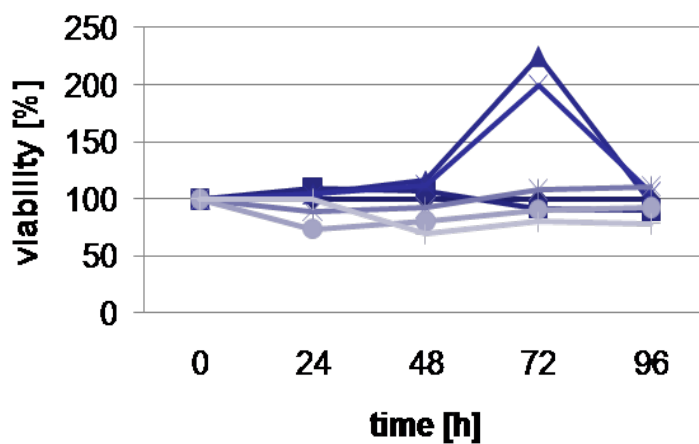
HaCaT

Figure 11 **MTT assay for HaCaT, SCC056, SCC114, and SCC116 during 96h of IL-6 treatment (5ng/mL to 160ng/mL).** Each point represents the mean of one triplicate normalized to the PBS control (100%) at each timepoint. Throughout the cell lines, viability stayed constant. A peak in HaCaT at 72h was noticed.

None of these cell lines experienced any major cell death. The only deviation noticed was a slight increase in proliferation in the HaCaT cell line at IL-6 concentration of 10 and 20ng/mL at 72h. This peak appeared most likely due to common MTT assay deviation and would need to be confirmed by repeated MTT assays. For further experiments, we decided on an effective IL-6 concentration of 100ng/mL, which has previously been used by others. (Foran et al., 2009)

3.4.3 Methylation Results with Pyrosequencing

The methylation status of the cell lines HaCaT, SCC056, SCC114, SCC116, and HCT116 after 96h of IL-6 treatment was evaluated via pyrosequencing and compared to the untreated steady-state values, which were both performed in the same pyrosequencing run (Table 10).

Table 10   Methylation status after 96h of IL-6 treatment (100ng/mL).
n.a.- data not available

Cell Lines	Treatment	MGMT [%]	RASSF 2-1 [%]	SOCS1 [%]	SFRP2 [%]	APC1A [%]
SCC056	untreated	1	1	83	80	2
	IL-6 96h	2	2	77	83	1
SCC114	untreated	2	12	3	2	93
	IL-6 96h	1	10	5	3	93
SCC116	untreated	1	12	4	2	91
	IL-6 96h	2	11	10	4	91
HaCaT	untreated	3	4	5	34	2
	IL-6 96h	2	4	4	27	2
HCT116	untreated	62	4	n.a.	93	5
	IL-6 96h	62	6	n.a.	93	3

No methylation changes were observed after IL-6 treatment in the selected genes except for minor changes in SOCS1 of SCC056 and SCC116.

In cancers, a coexistence of aberrant CpG hypermethylation and global hypomethylation has frequently been observed. Since the selected genes did not express any changes in CpG methylation after treatment with PMNs, H_2O_2, SNAP or IL-6, we performed pyrosequencing on the gene LINE-1, which has been proposed as a surrogate marker for global methylation (Figure 12).
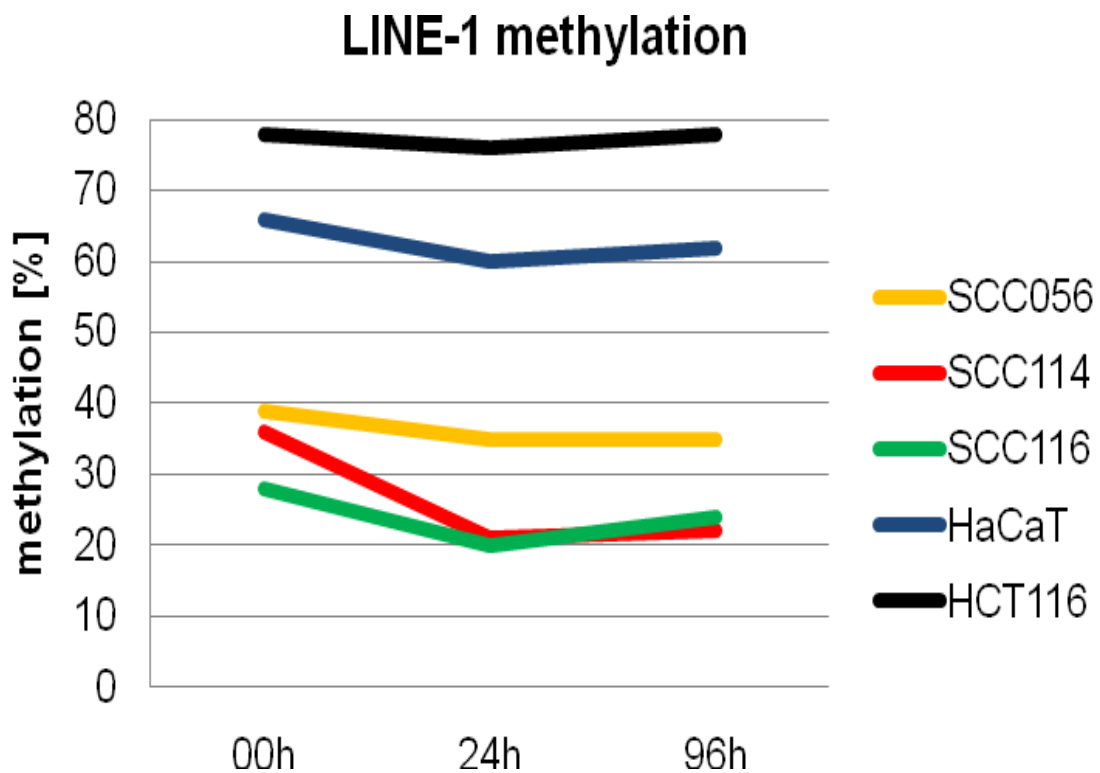
Figure 12 **LINE-1 methylation as a representation of the global methylation status.** The LINE-1 methylation level was evaluated by pyrosequencing. The DNA was tested upon 00h, 24h, and 96h of 100ng/mL IL-6 treatment in five different cell lines. Demethylation can be noticed upon IL-6 treatment in all cell lines except for HCT116.

Overall, IL-6 was able to induce significant LINE-1 hypomethylation (p=0.016). In addition, a significant quadratic trend (p=0.02) was measured, meaning that LINE-1 methylation at 24h is lower than at 00h or 96h. The data indicates that IL-6 may induce LINE-1 demethylation and thus represent global hypomethylation in the cell lines SCC056, SCC114, SCC116, and HaCaT. No change was observed in HCT116 upon IL-6 treatment. Treatment with 5-AZA (positive control), however, was able to induce strong global hypomethylation of -36%. (Data not shown.)

To compare the effects on global methylation, this experiment was also performed on HaCaT DNA from prior experiments. PMNs, H_2O_2, and SNAP also induced global DNA hypomethylation represented by LINE-1 demethylation of -5%,-12%, and -8%, respectively. (Data not shown.) All applied inflammatory in-vitro models caused LINE-1 demethylation.

3.4.4 Methylation Results with MS-MLPA

Since pyrosequencing is a reliable and unbiased method for detection of CpG methylation, we initially decided to use this method. However, the selection of genes is random and may not reflect the actual changes in the genome. Unfortunately the selected genes seemed to stay unaffected. This is probably why initially the experiments did not indicate any CpG island methylation changes.

As alternative method, the methylation status was analyzed by MS-MLPA. This technique has the advantage of screening several gene loci within one experiment and would widen the spectrum of our gene panel.

3.4.4.1 Reproducibility of MS-MLPA

Since MS-MLPA is a relatively new method and has only recently been introduced to our laboratory, the MS-MLPA kit was tested upon reproducibility of its results (Run 1) by repeating the sequencing with the same PCR products at

different concentrations (Run 2) and by repeating the entire MS-MLPA protocol (Run 3) for the cell line SCC056. Reproducibility was tested for SCC056 at 00h, 24h and 96h; however, data was similar and is only shown for SCC056 at 00h (Figure 13).
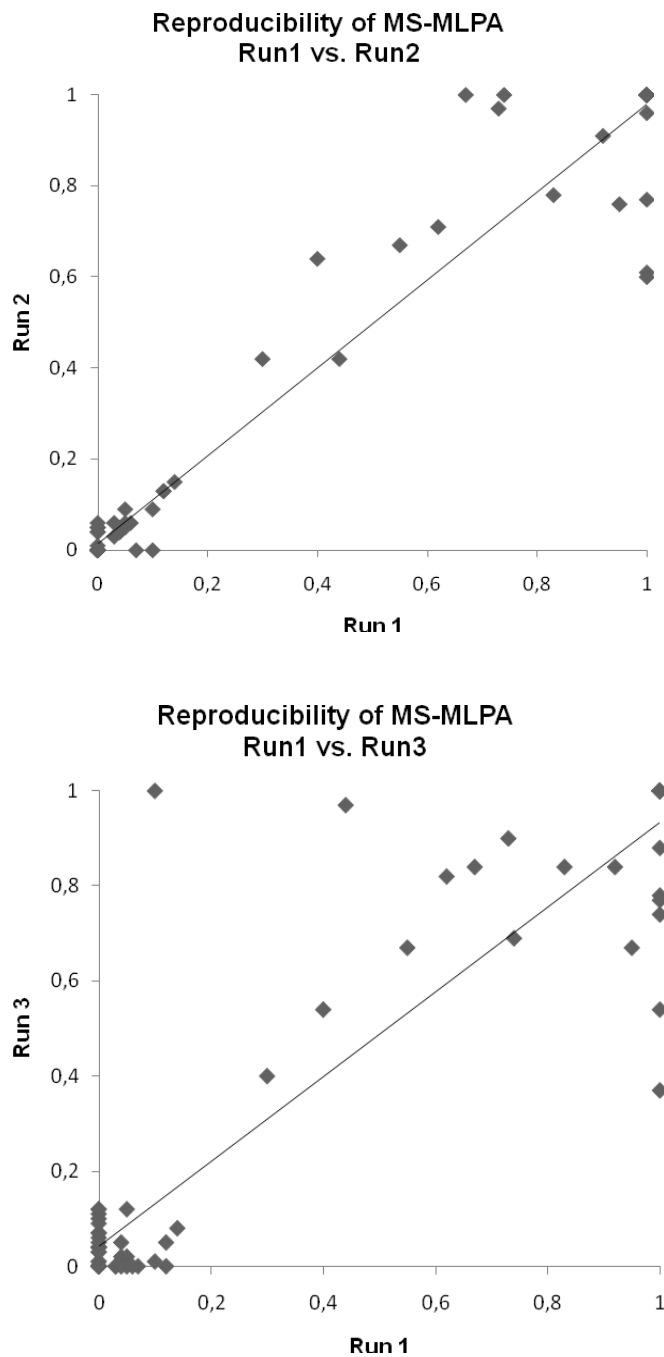
Figure 13　**MS-MLPA reproducibility of methylation analysis.** The figure shows the methylation data of untreated SCC056 probes. The

data from the first MS-MLPA experiment (Run 1) is compared to repeated sequencing (Run 2) and fully repeated MS-MLPA protocol (Run 3). Each point represents the methylation status of one MS-MLPA probe with ratios shown on the x-axis for Run1 and on the y-axis for either Run2 or Run3. The line represents the linear trendline.

Statistical analysis for SCC056 00h resulted in a Spearman r of 0.9701 and $p < 0.0001$ for Run 1 compared to Run 2 and a Spearman r of 0.8748 and $p < 0.0001$ for Run1 and Run3 due to a few outliers. The methylation status was cases well reproducible with MS-MLPA. In detail, even a change in methylation was detectable; especially the methylation change for PAX5 and PAX6 was well reproducible even in totally separate experiments. (Data not shown.)

3.4.4.2 Methylation Status Analysis

During analysis with the Coffalyser software, the results were normalized and a ratio for methylation was calculated for each probe. The methylation status was studied for 27 probes. Since MS-MLPA is a semi-quantitative method, the ratio of 0-0.29 stands for no methylation (green), the ratio 0.3-0.69 for hemimethylation (blue), and a ratio 0.7 and above for methylation (black). The results are shown in Figure 14.
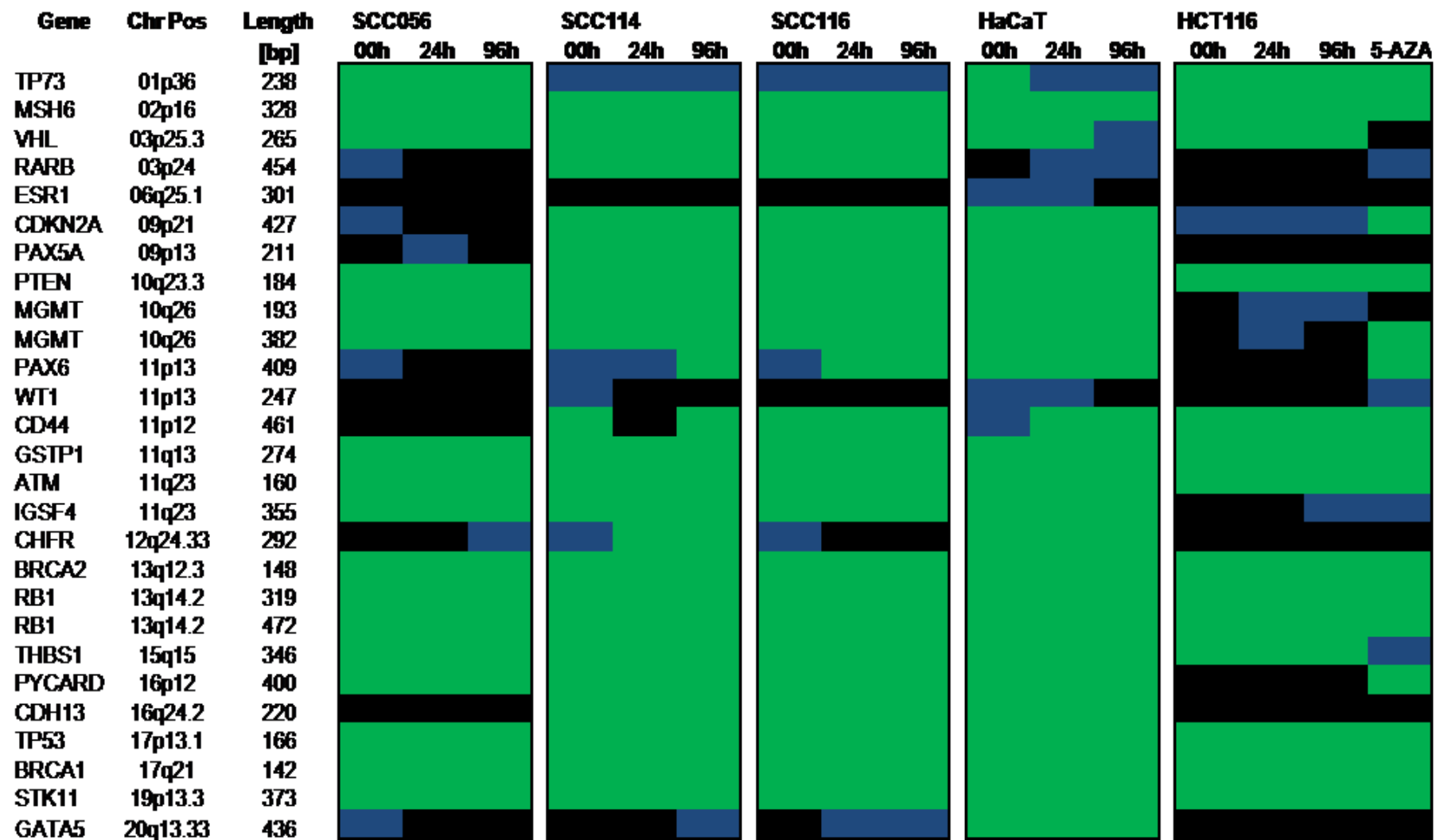
Figure 14   Methylation status analysis performed with MS-MLPA. The figure depicts the results of the cell lines SCC056, SCC114, SCC116, HaCaT, HCT116 comparing 00h versus 24h versus 96h IL-6 treatment (100ng/mL) and in case of HCT116 also 5-aza-2'deoxycytidine (5-AZA). Green coloring stands for no methylation (ratio 0-0.29), blue stands for hemimethylation (ratio 0.3-0.69) and black for methylation (ratio 0.7 and above). The Coffalyser analysis calculates the peak ratios of digested versus undigested samples after normalization and correction for sloping.

Upon IL-6, the oral cancer cell line SCC056 generally experienced CpG island hypermethylation. A change in methylation was noticed in the CpG islands of the genes RARB, CDKN2A, PAX5A, PAX6, CHFR, and GATA5. SCC114's methylation level changed in the genes PAX6, WT1, CD44, CHFR, and GATA5. In SCC116, the genes PAX6, CHFR, and GATA5 showed a change in methylation. The three investigated oral cancer cell lines had a change of three genes in common. These three genes, CHFR, GATA5, and PAX6, were selected to perform in-depth experiments to confirm the MS-MLPA results and investigate changes of the gene expression.

IL-6 was also able to change the CpG island methylation level in the mostly unmethylated immortalized skin keratinocyte cell line HaCaT. The effected genes were TP73, VHL, RARB, ESR1, WT1, and CD44. The colon cancer cell line HCT116 was strongly methylated at baseline and showed CpG methylation changes in both MGMT probes and IGSF4 upon IL-6 treatment. In comparison, 5-AZA treatment caused strong demethylation in multiple genes.

3.4.5 Methylation Results with SMART-MSP

To verify the results from MS-MLPA, the real-time PCR-based method SMART-MSP was considered appropriate due to its high accuracy, especially when compared to the commonly used MSP method. Due to the different initial DNA

amounts, values were normalized to COL2A1 and the artificially 100% methylated SssI-treated raji sample by the delta-delta c_T method.

Figure 15 depicts all methylation and gene expression results for CHFR, GATA5, and PAX6 for a good overview. Because of the difficulty comparing semi-quantitative (MS-MLPA) and quantitative (SMART-MSP, qRT-PCR) methods, we only compare trends. For MS-MLPA, a mean value was used to describe unmethylated (14.5%), hemimethylated (49.5%), and methylated (85.0%) levels. For SMART-MSP and qRT-PCR, the results for 24h treatment did not always perfectly blend in, so the general trend was determined by comparing 00h to 96h.
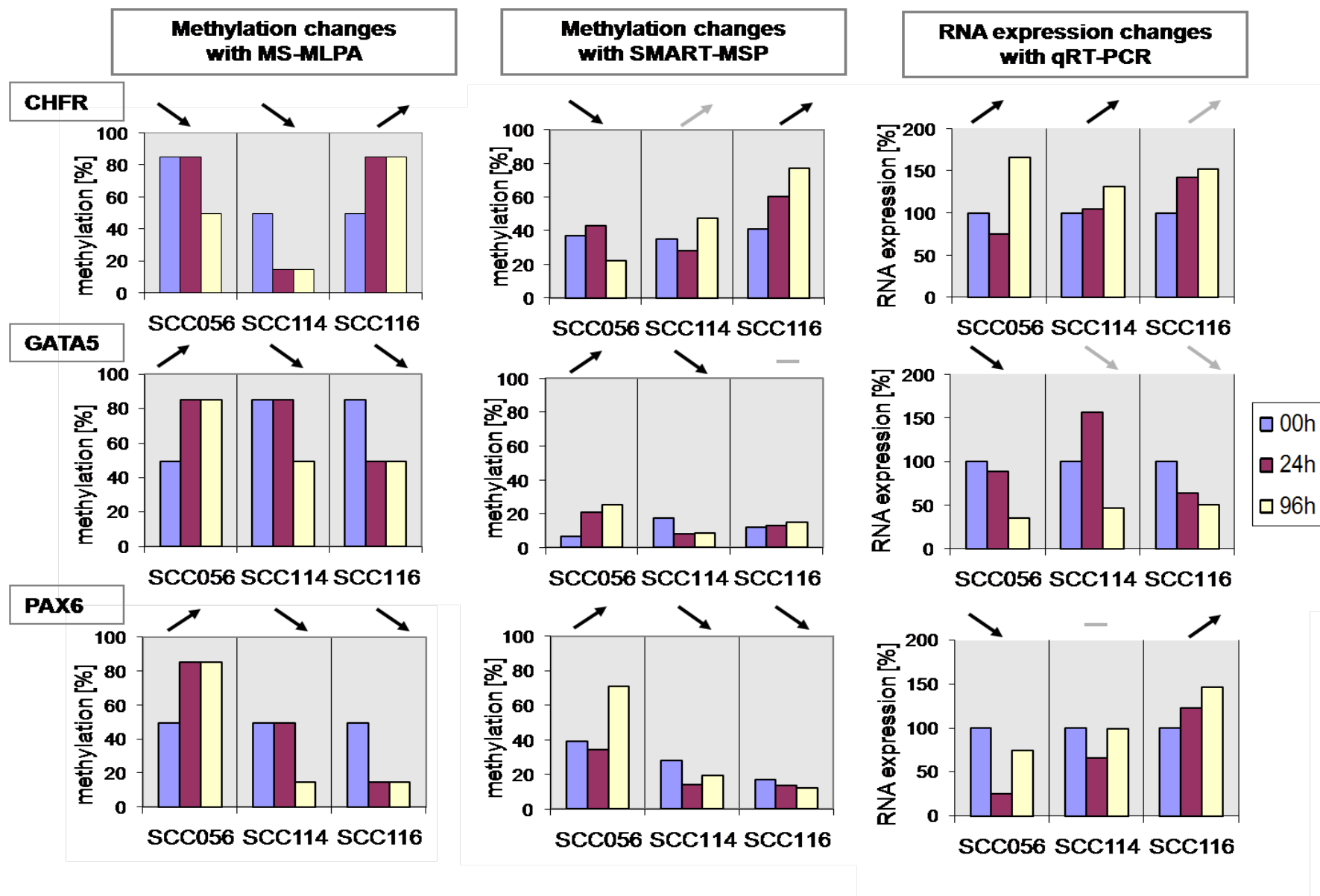
Figure 15   Methylation results and gene expression for CHFR, GATA5, and PAX6. The methylation levels were evaluated by MS-MLPA (left column) and SMART-MSP (center column). The gene expression was then evaluated for the same genes by qRT-PCR (right column). The data was collected for the oral cancer cell lines SCC056, SCC114, and SCC116 for 00h, 24h, and 96h of 100ng/mL IL-6 treatment. The arrows above each graph show the trend of hyper- versus hypomethylation or under- versus over-expression of the specific gene. A bar above the graph stands for no change due to IL-6. Black arrows indicate corresponding data comparing MS-MLPA with either the SMART-MSP or qRT-PCR results. Grey-colored trends stand for not correlating results in SMART-MSP or unexpected gene regulation in qRT-PCR.

We assume that the absolute methylation levels of SMART-MSP are not accurate, probably because of unsuccessful SssI treatment of the positive control and therefore incorrect normalization resulting in lower than actual methylation levels. However, for comparison and validation purposes these data were sufficient to show a trend of methylation change.

Except for CHFR in SCC114 and GATA5 in SCC116, there was a clear correlation for the changes in methylation between SMART-MSP and MS-MLPA. For most of the data, SMART-MSP confirmed the MS-MLPA data.

3.4.6 RNA Expression Data with qRT-PCR

Besides acknowledging the change in methylation, it is of biological importance to test for functional changes of gene and protein expression. Due to the different initial amounts of cDNA, each value was normalized to a housekeeping gene (β-actin) and the untreated values (100% gene expression assumed) by performing the delta-delta c_T method.

Taking SCC056 as an example, the results of MS-MLPA, SMART-MSP, and qRT-PCR correlate nicely (Figure 15). While CHFR is experiencing hypomethylation upon IL6, its mRNA expression is up-regulated. In GATA5 and PAX6, the methylation level is increased by IL-6 and the gene expression down-regulated. This inverse correlation between promoter methylation and gene expression does not have to match always perfectly, since enough hypo- or hypermethylation has to occur for an expression change to take place.

3.4.7 DNMT1 and DNMT3b Expression

Our hypothesis states that IL-6 as mediator of chronic inflammatory diseases can induce aberrant CpG hypermethylation of certain target genes. Current knowledge implies that an increase of DNMT activity induces such hypermethylation. Next, we investigated DNMT1 and DNMT3b expression levels in 00h versus 96h IL-6-treated cell lines via western blot (Figure 16).
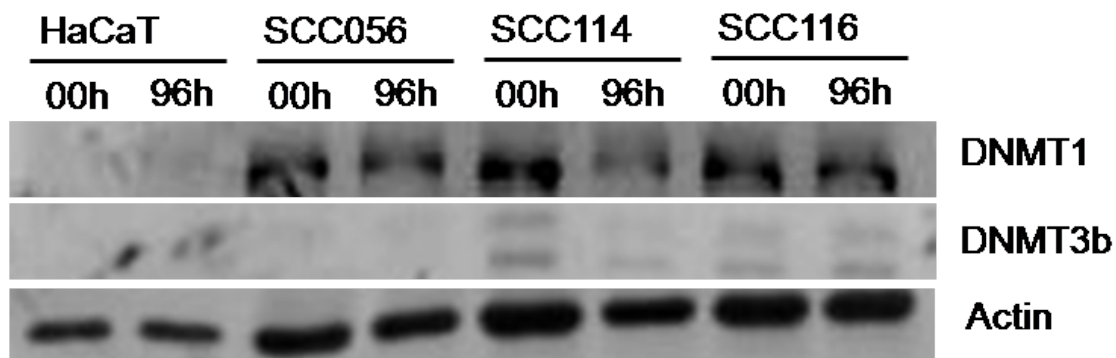
Figure 16   **DNMT1 (170-195kDa) and DNMT3b (96kDa) expression comparing 00h versus 96h of IL-6 treatment (100ng/mL).** Actin was used as loading control. There is no increase in DNMT1 or DNMT3b expression upon IL-6 treatment. However, the quality and the different loading amounts are not ideal in these blots.

After 96h of IL-6 treatment, there was neither a change in DNMT1 or DNMT3b protein expression.

Foran and colleagues recently demonstrated an increase in DNMT1 expression due to IL-6 treatment in HCT116 cells. (Foran et al., 2009) To test whether these data can be replicated in our laboratory, we repeated the experiments for HCT116 at similar conditions. The colon cancer cell line HCT116 was cultured with and without 100ng/mL IL-6 for 24h and 96h. A western blot was performed on nuclear extracts to test for changes in DNMT1 upon IL-6 treatment (Figure 17).
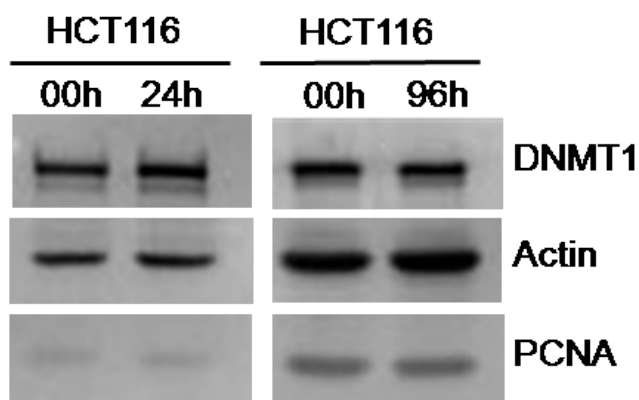
Figure 17   DNMT1 (170-195kDa) expression in nuclear extracts of HCT116 cells after 00h, 24h and 96h of IL-6 treatment (100ng/mL). Actin was used as general loading control and PCNA as nuclear loading control. No change in DNMT1 expression was observed.

Neither after 24h or 96h, a noticeably change in DNMT1 expression was observed. Thus, we were unable to reproduce the results by E. Foran.

4 Discussion

In this doctoral thesis, we tested the hypothesis that chronic inflammation of the oral cavity changes DNA methylation of certain promoters and thereby causes epigenetic expression changes of such genes. This would provide a field effect that enhances tumor formation and cancer development. Besides PMA-activated PMNs, we tested the effects of oxidative stress and nitrosative radicals as source of inflammatory mediators in cell culture. The major focus of this project, however, turned to IL-6-dependent tumor progression. With pyrosequencing, we were unable to detect biologically relevant methylation changes in our selected gene panel with any of the inflammatory mediators. With IL-6 treated DNA, we used further methodological approaches. We analyzed global hypomethylation, CpG island methylation changes, and according modifications of gene expression. Upon IL-6, we observed global hypomethylation, changes in the CpG island methylation of several genes and consequently aberrant gene expression.

4.1 Inflammatory Models Induce Global Hypomethylation

The major finding of this project is that all forms of tested inflammation PMNs, H_2O_2, SNAP, and IL-6 induced global hypomethylation represented by LINE-1 pyrosequencing data.

In cancer cells, two phenomena have generally been observed: genome-wide hypomethylation and/ or aberrant CpG island hypermethylation. Genome-wide DNA hypomethylation is seen in correlation with genomic instability and is known to contribute to carcinogenesis. (Ogino et al., 2008) In colorectal cancer, it has been proposed that LINE-1 hypomethylation or global hypomethylation is

associated with CIN. (Ogino et al., 2008) On the contrary, LINE-1 hypermethylation or global hypermethylation is proven to be associated with CIMP and MSI. (Ogino et al., 2008) Repetitive DNA sequences may contribute to tumorigenesis by causing CIN and oncogene expression. (Choi et al., 2009)

IL-6 induced LINE-1 hypomethylation in SCC056, SCC114, SCC116, and HaCaT, all of which had been tested for the presence of an IL-6-dependent phosphorylation of STAT3. For the oral cancer cell lines, the LINE-1 methylation level decreased by at least 10%. From this data, we conclude that IL-6 causes global hypomethylation (p=0.016). In a smaller but still distinct extent, PMNs, H_2O_2, and SNAP also induced global hypomethylation. It is currently not clear whether STAT3 is involved and why this effect was observed in its strongest form at 24h rather than 96h.

4.2 IL-6 Alters CpG Island Methylation

For detailed CpG island methylation analysis, MS-MLPA was performed with a selected tumor suppressor gene panel to detect changes in CpG island methylation. MS-MLPA gives detailed insight into CpG island methylation profile. Treatment with IL-6 modified the CpG methylation pattern of several genes in all tested cell lines. Alterations were observed as both CpG hyper- and hypomethylation.

Worsham and colleagues performed MS-MLPA applying a different gene panel on head and neck cancer cell lines. They observed promoter hypermethylation due to disease progression from primary to recurrent or metastatic disease. Hypermethylation of the genes KLK10 and IGSF4, TIMP3 and FHIT, and TP73 occurred in the cell lines UM-SCC-11B, UM-SCC-17B, and UM-SCC-81B, respectively. Therefore, it seems plausible that our in-vitro results reflect an in-vivo condition during tumor development.

Viet and Schmidt performed a methylation-specific OSCC screening using the Illumina Golden Gate methylation array to detect the gene loci which are frequently methylated in preoperative saliva and tissue, but unmethylated in postoperative saliva of OSCC patients and saliva of healthy subjects. The array, which allows screening of 1,505 CpG loci in 807 genes, detected a distinctive gene panel consisting of 41 gene loci from 34 genes. Most of those genes are involved in cell signaling, cell adhesion, cell proliferation, and differentiation indicating that these genes have functional importance to tumor development. This study also described methylation changes of WT1 and ESR1, which were part of the gene panel. (Viet and Schmidt, 2008) Promoter hypermethylation of WT1 and ESR1 participates in the stepwise tumor progression in the oral cavity. These observations are consistent with our own. While the oral cancer cell lines SCC056 and SCC116 were already fully methylated for WT1, IL-6 was able to increase from hemimethylation to methylation in SCC114. The same WT1 methylation increase was noticed in HaCaT. For ESR1, the oral cancer cell lines were already fully methylated, but an increase from hemimethylation to methylation was detected in HaCaT as well.

Since we detected cases of CpG island methylation changes applying MS-MLPA, we assumed to see a change in DNMT1 expression by western blot. In order to detect overall CpG island hypermethylation, the expression of the methylating enzymes DNMT1 and DNMT3b was assessed but no increase was noticed upon IL-6. However, this method might not be sensitive enough to detect small changes. Also, the amount of DNMT does not necessarily need to correlate with the level of activity. There can be little but highly active DNMTs. As the DNA-bound DNMTs are considered to be currently active, it might be more accurate to look for DNA-bound, rather than nuclear DNMTs.

Our western blots did not detect any change in DNMT1 and DNMT3b expression with IL-6 treatment. However, several publications present IL-6-induced DNMT1 overexpression in several different cell lines. Hodge et al published that human multiple myeloma cells treated with IL-6 showed an

increased DNMT1 expression resulting in decreased p53 expression. (Hodge et al., 2005) Furthermore, they noticed that IL-6 controls the expression of the DNMT gene and various transcription factors in human erythroleukemia cells. (Hodge et al., 2001) By activating the AKT pathway, IL-6 served as anti-apoptotic factor promoting tumorigenesis. (Hodge et al., 2005) In cholangiocarcinoma, Webhe et al. demonstrated that IL-6 promotes tumor proliferation by promoter hypermethylation. (Wehbe et al., 2006) In pancreatic cancer, IL-6 causes epigenetic silencing of SOCS1 through aberrant hypermethylation which blocks this important negative feedback loop of the JAK/ STAT-pathway. (Fukushima et al., 2003) However, both groups, Webhe et al and Fukushima et al, did not demonstrate any changes of DNMTs upon IL-6 treatment. By immunohistochemistry, Foran et al. described a DNMT1 overexpression in inflammation-associated colorectal cancer, both in the tumor tissue and the peritumoral stroma. When treating HCT116 cells with 100ng/mL IL-6 for 6, 24, and 48h, they detected an increased DNMT1 expression by western blot of the nuclear extracts. They further proposed that IL-6 stabilizes the exogenous DNMT1 expression via AKT-pathway mediation. The methylation array showed promoter methylation after 48h treatment with 100ng/mL IL-6 in selected tumor suppressor genes (IL-4, Maspin, IRF-7, PAI-1) resulting in decreased gene expression and reversible expression after 5-AZA treatment. (Foran et al., 2009)

4.3 IL-6 Induces CHFR, GATA5, and PAX6 CpG Methylation Changes

To identify some of the genes involved in OSCC tumorigenesis, we performed MS-MLPA to detect the methylation status of a selected tumor suppressor gene panel. Three genes CHFR, GATA5, and PAX6 were selected from this panel because they showed widespread methylation changes in OSCC cell lines. MS-MLPA is a semi-quantitative method distinguishing between unmethylated, hemimethylated, and methylated. For verification purposes, SMART-MSP was introduced to test methylation changes of CHFR, GATA5, and PAX6. SMART-

MSP is a quantitative method giving exact methylation percentages as results. For evaluation purpose, we only compared between increase and decrease in CpG methylation induced by IL-6. MS-MLPA and SMART-MSP showed comparable trends of methylation changes. In 7 out of 9 cases, the MS-MLPA data was confirmed by SMART-MSP.

Aberrant promoter hypermethylation of the CHFR gene has recently been described in context with oral carcinogenesis. In one study, aberrant promoter hypermethylation was found in 34.7% (17 of 49) of OSCC tumor samples. The adjacent normal mucosa was examined for CHFR methylation, but only 7.7% (1 of 13) were identified with hypermethylation. (Baba et al., 2009) These observations suggest that methylation of CHFR is closely linked to oral carcinogenesis. No reports have been published so far on GATA5 or PAX6 in relation to oral cancer.

4.4 IL-6 Causes CHFR, GATA5, and PAX6 Gene Expression Changes

Promoter methylation is a known regulator of gene expression. But changes in methylation do not necessarily mean changes in gene expression. For this reason, we measured mRNA expression levels of the selected genes CHFR, GATA5, and PAX6 by qRT-PCR.

A good inverse correlation between CpG methylation and gene expression is observed in SCC056 cells. The methylation changes follow the same trends using MS-MLPA and SMART-MSP, while these results are indirectly correlated with the RNA expression. Therefore, we conclude that aberrant CpG island hypermethylation induced by IL-6 is able to down-regulate gene expression, while IL-6 induced hypomethylation up-regulates such. In the cell lines SCC114 and SCC116, these results were not as consistent. No previous publications have investigated the gene expression of CHFR, GATA5, and PAX6 in OSCC.

4.5 Shortcomings

Chronic oral inflammation is an independent risk factor for OSCC. It is current understanding that inflammation has only a modest contribution to carcinogenesis compared to the major risk factors alcohol and tobacco. Both alcohol and tobacco induce, however, chronic inflammation themselves. Thus, it is not clear whether it is the toxic or the inflammatory response to alcohol or tobacco use which actually drives tumor formation in the oral cavity.

This present study applied three different in-vitro models to simulate an inflammatory environment. Due to the in-vitro setting, one might argue that these selected agents and short-term treatments might rather simulate an acute model of inflammation. The agents would never occur at such high concentrations in a clinical situation and might therefore not cause these strong tumor promoting effects. As example, the tumor necrosis factor (TNF) is a major mediator of diverse inflammatory responses. At high local dosage, it destroys the tumor's vasculature, but at low chronic dosage, it promotes tumorigenesis by inhibiting apoptosis and by supporting tissue remodeling and stromal progression. (Balkwill and Mantovani, 2001)

Due to the lack of telomerase in healthy cells, "normal cell lines" of the oral cavity do not exist. Also the selection of the immortalized human keratinocyte cell line HaCaT does not entirely reflect the clinical oral setting. Oral fibroblasts, although limited in replication, are mesenchymal cells and undergo different malignant transformation than epithelial cells. For these reasons, the results of HaCaT and primary oral fibroblasts are limited in interpretation, since neither of these cell lines falls into the category "healthy oral keratinocyte lineage". However, this was an attempt to resemble the clinical scenario.

4.6 Perspectives

4.6.1 Future Diagnostics

The key to a better prognosis in terms of overall survival rate is the early detection and diagnosis of premalignant lesions and cancer tissue to remove smaller lesions with less invasive treatment necessary. Aberrant hypermethylation is an early event in tumorigenesis. Even the tumor surrounding tissue and premalignant lesions show signs of hypermethylation (field effect). Using hypermethylation as a diagnostic and prognostic marker would therefore be a promising attempt for cancer screening with a methylation gene panel to detect premalignant or small OSCC formations. The evaluation of the methylation status implies the capability to be useful for early OSCC detection, monitoring and treatment. (Ha and Califano, 2006; Nakahara et al., 2006)

Besides serum analysis, saliva is being more and more investigated as a non-invasive tool for diagnostics. (Nakahara et al., 2006) The discovery of tumor-associated proteins, transcripts (mRNA), and microRNA in whole and supernatant saliva has lead to new anticipations for detection of OSCC. (Park et al., 2009) Studying the miRNA profile in saliva of 50 healthy versus 50 OSCC patients, Park et al observed that miRNA-200a and miRNA-125a were present at significantly reduced levels in OSCC patients. (Park et al., 2009) In primary OSCC tumor samples, miR-137 and miR-193a were identified as tumor suppressor miRNAs silenced by aberrant DNA hypermethylation. (Kozaki et al., 2008)

As valuable biomarker for oxidative DNA damage, 8-hydroxy-deoxyguanosine (8-OHdG) has been established. 8-OHdG is directly caused by ROS and considered a fingerprint of oxidative stress. The presence of 8-OHdG may lead to DNA mispairing during replication and point mutations. An increase in 8-OHdG is associated with premalignant lesions and OSCC. (Hooper et al., 2009)

The cytokines IL-6 and IL-8 have been proposed as OSCC biomarkers. Both mRNA and protein levels of IL-6 in serum and IL-8 in saliva were found significantly increased in OSCC patients compared to normal subjects. The protein level, assessed by ELISA, was used for ROC analysis to interpret their sensitivity and specificity. A combined detection of IL-6 and IL-8 would yield a sensitivity of 99% and a specificity of 90%. As the serum IL-6 levels have shown to decrease after treatment, this biomarker might be helpful for OSCC detection screening patients at risk, but also to monitor the success of treatment and disease recurrence of OSCC patients. (St John et al., 2004)

4.6.2 Future Therapeutic Concepts

Due to the disadvantages of today's surgical approach causing a significant loss in oral function like speaking or swallowing and often poor cosmetic outcomes, there is a significant need for innovations in OSCC treatment. Furthermore, the medical outcome in terms of survival rate has not improved much in the last few decades. Since the major focal points of this investigation were methylation and inflammation in OSCC, the author will therefore focus on these variables and how these can be affected by different treatment modalities.

4.6.2.1 Targeting Methylation

Epigenetic alterations are potentially reversible, early events during oral tumorigenesis. Epigenetic therapy has been suggested as potentially valuable in combination with chemotherapy and chemoprevention. For these reasons, epigenetics provide an attractive target for future therapy. New therapeutic intents focus on reversing epigenetics to restore normal gene function. (Esteller, 2002) In cancer tissue, promoter hypermethylation and global hypomethylation have regularly been observed to cause silencing of tumor suppressor genes and genomic instability. In its healthy state, the DNA shows mostly CpG hypomethylation and histone acetylation activating gene transcription. In aberrantly hypermethylated tumor tissue, the DNA is mostly hypermethylated by DNMTs and methyl-binding proteins, the histones are deacetylated by HDACs

or methylated by histone methyltransferases. Targets for therapy are preferably the regulating enzymes modifying the aberrantly heterochromatic regions. In order to reverse epigenetic abnormalities, researchers have worked on improving anti-cancer therapeutics like the DNMT inhibitors, which effectively reverse the tumorigenic process of DNA hypermethylation. (Hellebrekers et al., 2007) The goal of DNMT inhibition therapy is to restore normal methylation patterns by reactivating tumor suppressor genes and other genes crucial to normal cell functioning, and prevent the occurrence of further aberrant hypermethylation. (Yoo and Jones, 2006) Demethylating and histone acetylating agents were introduced moreover as combined drug cocktail. (Shaw, 2006) Worrisome, however, might be the toxicity of these medications when they're incorporated into normal cells. (Hodge et al., 2005)

In the category of DNA methylation inhibitors, we distinguish between nucleoside analogues and non-nucleoside analogues. Nucleoside analogues consist of a modified cytosine ring which is attached to a ribose or desoxyribose molecule. In the presence of a nucleoside analogue, the DNMT enzyme and the DNA constitute a covalent complex by incorporating the drug into the DNA strand. DNMT cannot be released from this binding and is therefore unable to move to further sites. Its effectiveness at low dosage and its low toxicity are some of the drug's advantages. However, the drug only causes a transient effect meaning that the aberrant methylation pattern will return to its former pattern after drug removal and cause the reappearance of aberrant cells. 5-AZA belongs to this group and has a very potent demethylating effect. 5-AZA is capable of reversing methylation by inhibiting DNMTs and causes non-specific global hypomethylation. (Esteller, 2002) First synthesized in the 1960s and clinically introduced in the 1970s as antitumor drugs, it has effective anti-cancer properties that induce cellular differentiation and reverse aberrant DNA hypermethylation. (Shaw, 2006; Yoo and Jones, 2006) In combination, HDAC inhibitors show a synergistic effect. (Shaw, 2006) As antioxidant, 5-AZA traps potentially harming free radicals. For effective treatment in the oral cavity, it would need to be applied locally. In contrast to the nucleoside analogues, the

non-nucleoside analogues inhibit DNMTs by binding directly to their catalytic region, therefore inactivating the enzyme without incorporation into the DNA strand. So far, only a few compounds of this category have been developed.

The general problem of DNMT inhibitors is the issue of loss of specificity: DNMT inhibitors cause a target-unspecific global demethylation reactivating methylation-silenced genes. This loss of specificity, however, might potentially further decrease the genome-wide levels of methylation and activate harmful oncogenes. (Yoo and Jones, 2006) Besides the demethylating agents mentioned above, natural compounds such as boswellic acid or curcumin have shown demethylating effects in several cancers and might therefore present a novel epigenetic therapy for OSCC (Culioli et al., 2003; Moiseeva et al., 2007).

Gene polymorphisms of DNMT3b (-149C>T and -579G>T) have shown statistical differences in survival rates. The homozygous genotypes are associated with an increased risk for the development of HNSCC. (Liu et al., 2008) It would be helpful to detect this population with these specific polymorphisms and develop different treatment strategies.

4.6.2.2 Targeting Inflammation

In order to reduce the risk for cancer caused by inflammation, we need to find a way to modify the host's inflammatory response by decreasing the tumor-promoting factors, but increasing tumor-suppressive properties. (Coussens and Werb, 2002) As mentioned in the introduction, anti-inflammatory long-term treatment using aspirin and NSAIDs decreases the risk to develop colon cancer by 40 to 50% and it might also prevent lung, esophageal, and gastric cancer. (Coussens and Werb, 2002) For the purpose of solemnly cancer prevention, however, long-term systemic anti-inflammatory agents seem unreasonable. However, for oral cancer treatment a local application may be considered.

Immunotherapy will be one hope in future therapeutics. It appears most promising as antibody therapy or vaccine in an adjuvant setting in patients with early-stage or premalignant OSCC. (Davidson et al., 2009) Especially molecular targeted therapy might prove useful due to its higher therapeutic index and lower toxicity. (Choi and Myers, 2008) Mouse monoclonal antibodies to IL-6 may be used for IL-6 antagonism. In a preliminary study with ten myeloma patients, IL-6 antagonists decreased C-reactive protein, reduced IL-6 production, and resolved low-grade fever. (Balkwill and Mantovani, 2001; Bromberg and Wang, 2009) This drug is currently in clinical development for rheumatoid arthritis.

4.6.3 Future Research

With over 100,000 deaths per year worldwide due to OSCC, there is a serious need to develop alternatives for early detection and treatment. In order to improve survival, we need to encourage basic dental research to achieve a better fundamental understanding of the pathogenesis of OSCC.

Further research is needed for a better pathomechanistic understanding of OSCC development. One topic of future investigations could be the identification of the pathways by which chronic inflammation causes oral cancer. New projects could investigate the dimensions of inflammation's effects on tumorigenesis compared to tobacco and alcohol as the main risk factors. As the hamster cheek pouch is the best represented in-vivo animal model for OSCC, this system might be a good way to investigate chronic inflammation and its effects in the oral cavity. Also, the bacterial flora of the oral cavity needs to be investigated for its involvement in OSCC tumorigenesis. The proper information on the mechanisms by which OSCC develops might open new avenues for the primary prevention and treatment of oral cancer.

Future research on selecting reliable biomarkers for detection of oral premalignancies and OSCC is on its way. A reliable panel of biomarkers needs

to be established and a simple methylation test developed. A method similar to MS-MLPA would be preferred due to its simple application and quick analysis. Ideally, this test should be introduced into the dentist's daily routine to screen high-risk patients and monitor OSCC patients after therapy.

Also clinical trials are needed to investigate the applications and effects of epigenetic therapies and their use in OSCC treatment. Due to the easy accessibility of the oral cavity, it might be practical to develop oral patches, chewing gums or rinsing solutions containing therapeutic agents.

4.7 Conclusion

To this point of knowledge, inflammation and methylation are both related to oral tumorigenesis, however inflammation-driven effects on methylation have not yet been studied in oral cancer. This project investigated whether chronic inflammation alters the DNA methylation profile.

Herein, we demonstrate that inflammation represented by PMNs, H_2O_2, SNAP, and IL-6 induces global hypomethylation. IL-6 was specifically able to alter the CpG island methylation level of certain genes and modify their gene expression. The information gained from this project might help to further investigate inflammation's role as risk factor in OSCC and include anti-inflammatory agents into future therapeutic strategies to preserve the genome's physiologic methylation status.

5 Summary

In the present study, we investigated whether chronic inflammation may alter the global or CpG methylation pattern causing oral tumorigenesis by silencing of tumor suppressor genes.

For a wide approach, we presented three different in-vitro models to simulate an inflammatory environment: inflammatory cells (PMNs), oxidative and nitrosative stress (H_2O_2, SNAP), and direct pro-inflammatory stimulus via IL-6. We measured the ability to alter DNA methylation in non-cancer and oral cancer cell lines with pyrosequencing, MS-MLPA, and SMART-MSP. The gene expression was analyzed by qRT-PCR. The DNMT1 and DNMT3b expression was assessed by Western Blot.

Our major finding was that all three inflammatory models caused LINE-1 demethylation which can be interpreted as global DNA hypomethylation. Attempts to search for methylation changes with random tumor-associated gene selection by pyrosequencing failed. Upon a broader approach, CpG promoter methylation changes were observed in several tumor suppressor genes upon IL-6. The selected genes CHFR, GATA5, and PAX6 altered gene expression upon change in CpG methylation. Western blot did not detect any increase in DNMT1 and DNMT3b expression.

In conclusion, we identified that inflammation induces global DNA hypomethylation. The inflammatory mediator IL-6 changed the aberrant CpG island methylation profile resulting in altered expression of tumor-associated genes. Our observations closely link inflammation to epigenetic changes, which may contribute to oral carcinogenesis.

6 Legends

6.1 Index of Figures

6.2 Index of Tables

6.3 Index of Abbreviations

Abbreviation	Full description
5-AZA	5-aza-2'-deoxycytidine
8-OHdG	8-hydroxy-deoxyguanosine
8-oxodG	8-oxo-7,8-dihydro-2'-deoxyguanosine
APC1A	adenomatous polyposis coli 1A
cDNA	complementary DNA
CIMP	CpG island methylator phenotype
CIN	chromosomal instability
COX	cyclooxygenase
DNMT	DNA methyltransferase
FBS	fetal bovine serum
H_2O_2	hydrogen peroxide
HDAC	histone deacetylase
HNSCC	head and neck squamous cell carcinoma
HPP1	hyperplastic polyposis protein 1
IL	interleukin
iNOS	inducible isoform of nitric oxide synthase
JAK	Janus kinase
LINE-1	long interspersed nucleotide element-1
LOH	loss of heterozygosity
MGMT	O6-methylguanine DNA methyltransferase
miRNA	microRNA
mRNA	messenger RNA
MSI	microsatellite instability
MTT	3-(4,5-dimethyl-2-thiazolyl)-2,5-diphenyl-2H-tetrazolium bromide
NO	nitric oxide
NSAID	nonsteroidal anti-inflammatory drug
OSCC	oral squamous cell carcinoma
p16	cyclin-dependent kinase inhibitor 2A (CDKN2A)
PBMC	peripheral blood mononuclear cell

PHA	phytohaemagglutinin
PMA	phorbol 12-myristate 13-acetate
PMN	polymorphonuclear cell
qPCR	quantitative PCR (real time)
qRT-PCR	quantitative reverse transcriptase PCR
RASSF 2-1	Ras association domain family 2-1
RNS	reactive nitrogen species
ROS	reactive oxygen species
SAM-e	S-adenosyl- L-methionine
SFRP2	secreted frizzled-related protein 2
(s)IL-6R	(soluble) interleukin-6 receptor
SMART-MSP	sensitive melting analysis after real-time methylation specific PCR
SNAP	S-nitroso-N-acetyl-DL-penicillamine
SOCS1	suppressor of cytokine signaling 1
STAT	signal transducer and activator of transcription
TNF	tumor necrosis factor
VEGF	vascular endothelial growth factor

6.4 References

Alexander,W.S., Starr,R., Fenner,J.E., Scott,C.L., Handman,E., Sprigg,N.S., Corbin,J.E., Cornish,A.L., Darwiche,R., Owczarek,C.M., Kay,T.W., Nicola,N.A., Hertzog,P.J., Metcalf,D., and Hilton,D.J. (1999). SOCS1 is a critical inhibitor of interferon gamma signaling and prevents the potentially fatal neonatal actions of this cytokine. Cell *98*, 597-608.

Baba,S., Hara,A., Kato,K., Long,N.K., Hatano,Y., Kimura,M., Okano,Y., Yamada,Y., and Shibata,T. (2009). Aberrant promoter hypermethylation of the CHFR gene in oral squamous cell carcinomas. Oncol. Rep. *22*, 1173-1179.

Baez,A. (2008). Genetic and environmental factors in head and neck cancer genesis. J. Environ. Sci. Health C. Environ. Carcinog. Ecotoxicol. Rev. *26*, 174-200.

Bagan,J.V. and Scully,C. (2008). Recent advances in Oral Oncology 2007: Epidemiology, aetiopathogenesis, diagnosis and prognostication. Oral Oncology *44*, 103-108.

Balkwill,F. and Mantovani,A. (2001). Inflammation and cancer: back to Virchow? Lancet *357*, 539-545.

Bromberg,J. and Darnell,J.E., Jr. (2000). The role of STATs in transcriptional control and their impact on cellular function. Oncogene *19*, 2468-2473.

Bromberg,J. and Wang,T.C. (2009). Inflammation and cancer: IL-6 and STAT3 complete the link. Cancer Cell *15*, 79-80.

Bui,J.D. and Schreiber,R.D. (2007). Cancer immunosurveillance, immunoediting and inflammation: independent or interdependent processes? Curr. Opin. Immunol. *19*, 203-208.

Calo,V., Migliavacca,M., Bazan,V., Macaluso,M., Buscemi,M., Gebbia,N., and Russo,A. (2003). STAT proteins: from normal control of cellular events to tumorigenesis. J. Cell Physiol *197*, 157-168.

Campregher,C., Goel,A., Boland,C.R., and Gasche,C. (2009). Activated Neutrophils Induce DNA Methylation in Colon Epithelial Cells By Up-Regulating De-Novo DNA Methyltransferases DNMT3A and DNMT3B. Gastroenterology *136*, A-302.

Campregher,C., Luciani,M.G., and Gasche,C. (2008). Activated neutrophils induce an hMSH2-dependent G2/M checkpoint arrest and replication errors at a (CA)13-repeat in colon epithelial cells. Gut *57*, 780-787.

Chaiyarit,P., Ma,N., Hiraku,Y., Pinlaor,S., Yongvanit,P., Jintakanon,D., Murata,M., Oikawa,S., and Kawanishi,S. (2005). Nitrative and oxidative DNA damage in oral lichen planus in relation to human oral carcinogenesis. Cancer Sci. *96*, 553-559.

Chakravarti,N., Myers,J.N., and Aggarwal,B.B. (2006). Targeting constitutive and interleukin-6-inducible signal transducers and activators of transcription 3 pathway in head and neck squamous cell carcinoma cells by curcumin (diferuloylmethane). Int. J. Cancer *119*, 1268-1275.

Cheng,J.C., Matsen,C.B., Gonzales,F.A., Ye,W., Greer,S., Marquez,V.E., Jones,P.A., and Selker,E.U. (2003). Inhibition of DNA methylation and reactivation of silenced genes by zebularine. J. Natl. Cancer Inst. *95*, 399-409.

Choi,S. and Myers,J.N. (2008). Molecular pathogenesis of oral squamous cell carcinoma: implications for therapy. J Dent. Res. *87*, 14-32.

Choi,S.H., Worswick,S., Byun,H.M., Shear,T., Soussa,J.C., Wolff,E.M., Douer,D., Garcia-Manero,G., Liang,G., and Yang,A.S. (2009). Changes in DNA methylation of tandem DNA repeats are different from interspersed repeats in cancer. Int. J. Cancer *125*, 723-729.

Clark,S.J., Harrison,J., Paul,C.L., and Frommer,M. (1994). High sensitivity mapping of methylated cytosines. Nucleic Acids Res. *22*, 2990-2997.

Coussens,L.M. and Werb,Z. (2002). Inflammation and cancer. Nature *420*, 860-867.

Culioli,G., Mathe,C., Archier,P., and Vieillescazes,C. (2003). A lupane triterpene from frankincense (Boswellia sp., Burseraceae). Phytochemistry *62*, 537-541.

Davidson,H.C., Leibowitz,M.S., Lopez-Albaitero,A., and Ferris,R.L. (2009). Immunotherapy for head and neck cancer. Oral Oncol. *45*, 747-751.

de Oliveira,M.V., de Carvalho Fraga,C.A., Gomez,R.S., and Paula,A.M. (2009). Immunohistochemical expression of interleukin-4, -6, -8, and -12 in inflammatory cells in surrounding invasive front of oral squamous cell carcinoma. Head Neck.

Duffy,S.A., Taylor,J.M., Terrell,J.E., Islam,M., Li,Y., Fowler,K.E., Wolf,G.T., and Teknos,T.N. (2008). Interleukin-6 predicts recurrence and survival among head and neck cancer patients. Cancer *113*, 750-757.

Esteller,M. (2002). CpG island hypermethylation and tumor suppressor genes: a booming present, a brighter future. Oncogene *21*, 5427-5440.

Foran,E., Garrity-Park,M., Mureau,C., Smyrk,T., Limburg,P., and Egan,L. (2009). Interleukin-6 Links Colonic Inflammation and Tumorigenesis Through DNA Methyltransferase-1-Mediated Epigenetic Gene Silencing. Gastroenterology *136*, A-463-A-464.

Fukushima,N., Sato,N., Sahin,F., Su,G.H., Hruban,R.H., and Goggins,M. (2003). Aberrant methylation of suppressor of cytokine signalling-1 (SOCS-1) gene in pancreatic ductal neoplasms. Br. J. Cancer *89*, 338-343.

Gomes,C.C. and Gomez,R.S. (2008). MicroRNA and oral cancer: future perspectives. Oral Oncol. *44*, 910-914.

Ha,P.K. and Califano,J.A. (2006). Promoter methylation and inactivation of tumour-suppressor genes in oral squamous-cell carcinoma. Lancet Oncol. *7*, 77-82.

Hamilton,J.P., Sato,F., Greenwald,B.D., Suntharalingam,M., Krasna,M.J., Edelman,M.J., Doyle,A., Berki,A.T., Abraham,J.M., Mori,Y., Kan,T., Mantzur,C., Paun,B., Wang,S., Ito,T., Jin,Z., and Meltzer,S.J. (2006). Promoter methylation and response to chemotherapy and radiation in esophageal cancer. Clin. Gastroenterol. Hepatol. *4*, 701-708.

Hanahan,D. and Weinberg,R.A. (2000). The hallmarks of cancer. Cell *100*, 57-70.

Hellebrekers,D.M.E.I., Griffioen,A.W., and van Engeland,M. (2007). Dual targeting of epigenetic therapy in cancer. Biochimica et Biophysica Acta-Reviews on Cancer *1775*, 76-91.

Herman,J.G., Graff,J.R., Myohanen,S., Nelkin,B.D., and Baylin,S.B. (1996). Methylation-specific PCR: a novel PCR assay for methylation status of CpG islands. Proc. Natl. Acad. Sci. U. S. A *93*, 9821-9826.

Hodge,D.R., Peng,B., Cherry,J.C., Hurt,E.M., Fox,S.D., Kelley,J.A., Munroe,D.J., and Farrar,W.L. (2005). Interleukin 6 supports the maintenance of p53 tumor suppressor gene promoter methylation. Cancer Res. *65*, 4673-4682.

Hodge,D.R., Xiao,W., Clausen,P.A., Heidecker,G., Szyf,M., and Farrar,W.L. (2001). Interleukin-6 regulation of the human DNA methyltransferase (HDNMT) gene in human erythroleukemia cells. J. Biol. Chem. *276*, 39508-39511.

Hooper,S.J., Wilson,M.J., and Crean,S.J. (2009). Exploring the link between microorganisms and oral cancer: a systematic review of the literature. Head Neck *31*, 1228-1239.

Imai,T., Toyota,M., Suzuki,H., Akino,K., Ogi,K., Sogabe,Y., Kashima,L., Maruyama,R., Nojima,M., Mita,H., Sasaki,Y., Itoh,F., Imai,K., Shinomura,Y., Hiratsuka,H., and Tokino,T. (2008). Epigenetic inactivation of RASSF2 in oral squamous cell carcinoma. Cancer Sci. *99*, 958-966.

Ishida,E., Nakamura,M., Ikuta,M., Shimada,K., Matsuyoshi,S., Kirita,T., and Konishi,N. (2005). Promotor hypermethylation of p14(ARF) is a key alteration for progression of oral squamous cell carcinoma. Oral Oncology *41*, 614-622.

Ishihara,K. and Hirano,T. (2002). IL-6 in autoimmune disease and chronic inflammatory proliferative disease. Cytokine Growth Factor Rev. *13*, 357-368.

Jemal,A., Siegel,R., Ward,E., Hao,Y., Xu,J., and Thun,M.J. (2009). Cancer statistics, 2009. CA Cancer J. Clin. *59*, 225-249.

Jones,S.A. (2005). Directing transition from innate to acquired immunity: defining a role for IL-6. J. Immunol. *175*, 3463-3468.

Jones,S.A., Richards,P.J., Scheller,J., and Rose-John,S. (2005). IL-6 transsignaling: the in vivo consequences. J. Interferon Cytokine Res. *25*, 241-253.

Katakura,A., Kamiyama,I., Takano,N., Shibahara,T., Muramatsu,T., Ishihara,K., Takagi,R., and Shouno,T. (2007). Comparison of salivary cytokine levels in oral cancer patients and healthy subjects. Bull. Tokyo Dent. Coll. *48*, 199-203.

Kato,K., Hara,A., Kuno,T., Mori,H., Yamashita,T., Toida,M., and Shibata,T. (2006). Aberrant promoter hypermethylation of p16 and MGMT genes in oral squamous cell carcinomas and the surrounding normal mucosa. J. Cancer Res. Clin. Oncol. *132*, 735-743.

Kim,B.H., Cho,N.Y., Shin,S.H., Kwon,H.J., Jang,J.J., and Kang,G.H. (2009). CpG island hypermethylation and repetitive DNA hypomethylation in premalignant lesion of extrahepatic cholangiocarcinoma. Virchows Arch.

King,C. and Scott-Horton,T. (2008). Pyrosequencing: a simple method for accurate genotyping. J. Vis. Exp.

Kozaki,K., Imoto,I., Mogi,S., Omura,K., and Inazawa,J. (2008). Exploration of tumor-suppressive microRNAs silenced by DNA hypermethylation in oral cancer. Cancer Res. *68*, 2094-2105.

Kristensen,L.S., Mikeska,T., Krypuy,M., and Dobrovic,A. (2008). Sensitive Melting Analysis after Real Time- Methylation Specific PCR (SMART-MSP): high-throughput and probe-free quantitative DNA methylation detection. Nucleic Acids Res. *36*, e42.

Kudo,Y., Kitajima,S., Ogawa,I., Hiraoka,M., Sargolzaei,S., Keikhaee,M.R., Sato,S., Miyauchi,M., and Takata,T. (2004). Invasion and metastasis of oral cancer cells require methylation of E-cadherin and/or degradation of membranous beta-catenin. Clin. Cancer Res. *10*, 5455-5463.

Liu,Z., Wang,L., Wang,L.E., Sturgis,E.M., and Wei,Q. (2008). Polymorphisms of the DNMT3B gene and risk of squamous cell carcinoma of the head and neck: a case-control study. Cancer Lett. *268*, 158-165.

Mendes,R.A., Carvalho,J.F., and Waal,I. (2009). An overview on the expression of cyclooxygenase-2 in tumors of the head and neck. Oral Oncol. *45*, e124-e128.

Mithani,S.K., Mydlarz,W.K., Grumbine,F.L., Smith,I.M., and Califano,J.A. (2007). Molecular genetics of premalignant oral lesions. Oral Dis. *13*, 126-133.

Moiseeva,E.P., Almeida,G.M., Jones,G.D., and Manson,M.M. (2007). Extended treatment with physiologic concentrations of dietary phytochemicals results in altered gene expression, reduced growth, and apoptosis of cancer cells. Mol. Cancer Ther. *6*, 3071-3079.

MRC-Holland,M. (2009). SALSA MS-MLPA KIT ME002-A1 Tumor suppressor-2. Description Version 09 1-7.

Nagpal,J.K. and Das,B.R. (2003). Oral cancer: reviewing the present understanding of its molecular mechanism and exploring the future directions for its effective management. Oral Oncol. *39*, 213-221.

Nakahara,Y., Shintani,S., Mihara,M., Hino,S., and Hamakawa,H. (2006). Detection of p16 promoter methylation in the serum of oral cancer patients. Int. J. Oral Maxillofac. Surg. *35*, 362-365.

Nygren,A.O., Lens,S.I., and Carvalho,R. (2008). Methylation-specific multiplex ligation-dependent probe amplification enables a rapid and reliable distinction between male FMR1 premutation and full-mutation alleles. J. Mol. Diagn. *10*, 496-501.

Ogino,S., Kawasaki,T., Nosho,K., Ohnishi,M., Suemoto,Y., Kirkner,G.J., and Fuchs,C.S. (2008). LINE-1 hypomethylation is inversely associated with microsatellite instability and CpG island methylator phenotype in colorectal cancer. Int. J. Cancer *122*, 2767-2773.

Oliveira,L.R., Ribeiro-Silva,A., Costa,J.P., Simoes,A.L., Matteo,M.A., and Zucoloto,S. (2008). Prognostic factors and survival analysis in a sample of oral squamous cell carcinoma patients. Oral Surg. Oral Med. Oral Pathol. Oral Radiol. Endod. *106*, 685-695.

Park,N.J., Zhou,H., Elashoff,D., Henson,B.S., Kastratovic,D.A., Abemayor,E., and Wong,D.T. (2009). Salivary microRNA: discovery, characterization, and clinical utility for oral cancer detection. Clin. Cancer Res. *15*, 5473-5477.

Parkin,D.M., Pisani,P., and Ferlay,J. (1999). Estimates of the worldwide incidence of 25 major cancers in 1990. Int. J. Cancer *80*, 827-841.

Reshmi,S.C. and Gollin,S.M. (2005). Chromosomal instability in oral cancer cells. J. Dent. Res. *84*, 107-117.

Rhodus,N.L., Cheng,B., Myers,S., Miller,L., Ho,V., and Ondrey,F. (2005). The feasibility of monitoring NF-kappaB associated cytokines: TNF-alpha, IL-1alpha, IL-6, and IL-8 in whole saliva for the malignant transformation of oral lichen planus. Mol. Carcinog. *44*, 77-82.

Sahebjamee,M., Eslami,M., Atarbashimoghadam,F., and Sarafnejad,A. (2008). Salivary concentration of TNFalpha, IL1 alpha, IL6, and IL8 in oral squamous cell carcinoma. Med. Oral Patol. Oral Cir. Bucal. *13*, E292-E295.

Sappayatosok,K., Maneerat,Y., Swasdison,S., Viriyavejakul,P., Dhanuthai,K., Zwang,J., and Chaisri,U. (2009). Expression of pro-inflammatory protein, iNOS, VEGF and COX-2 in oral squamous cell carcinoma (OSCC), relationship with angiogenesis and their clinico-pathological correlation. Med. Oral Patol. Oral Cir. Bucal. *14*, E319-E324.

Sassano,P., Paparo,F., Ramieri,V., Colangeli,W., and Verdino,G. (2007). Interleukine-6 (IL-6) may be a link between myasthenia gravis and myoepithelioma of the parotid gland. Med. Hypotheses *68*, 314-317.

Schmezer,P. and Plass,C. (2008). [Epigenetic aspects in carcinomas of the head and neck]. HNO *56*, 594-602.

Scully,C. and Bagan,J.V. (2008). Recent advances in Oral Oncology 2007: Imaging, treatment and treatment outcomes. Oral Oncology *44*, 211-215.

Shaw,R. (2006). The epigenetics of oral cancer. Int. J. Oral Maxillofac. Surg. *35*, 101-108.

Shaw,R.J., Hall,G.L., Lowe,D., Bowers,N.L., Liloglou,T., Field,J.K., Woolgar,J.A., and Risk,J.M. (2007). CpG island methylation phenotype (CIMP) in oral cancer: associated with a marked inflammatory response and less aggressive tumour biology. Oral Oncol. *43*, 878-886.

Shibata,D.M., Sato,F., Mori,Y., Perry,K., Yin,J., Wang,S., Xu,Y., Olaru,A., Selaru,F., Spring,K., Young,J., Abraham,J.M., and Meltzer,S.J. (2002). Hypermethylation of HPP1 is associated with hMLH1 hypermethylation in gastric adenocarcinomas. Cancer Res. *62*, 5637-5640.

Shintani,S., Nakahara,Y., Mihara,M., Ueyama,Y., and Matsumura,T. (2001). Inactivation of the p14(ARF), p15(INK4B) and p16(INK4A) genes is a frequent event in human oral squamous cell carcinomas. Oral Oncology *37*, 498-504.

Sogabe,Y., Suzuki,H., Toyota,M., Ogi,K., Imai,T., Nojima,M., Sasaki,Y., Hiratsuka,H., and Tokino,T. (2008). Epigenetic inactivation of SFRP genes in oral squamous cell carcinoma. Int. J. Oncol. *32*, 1253-1261.

St John,M.A., Li,Y., Zhou,X., Denny,P., Ho,C.M., Montemagno,C., Shi,W., Qi,F., Wu,B., Sinha,U., Jordan,R., Wolinsky,L., Park,N.H., Liu,H., Abemayor,E., and Wong,D.T. (2004). Interleukin 6 and interleukin 8 as potential biomarkers for oral cavity and oropharyngeal squamous cell carcinoma. Arch. Otolaryngol. Head Neck Surg. *130*, 929-935.

Sturgis,E.M., Wei,Q., and Spitz,M.R. (2004). Descriptive epidemiology and risk factors for head and neck cancer. Semin. Oncol. *31*, 726-733.

Subbalekha,K., Pimkhaokham,A., Pavasant,P., Chindavijak,S., Phokaew,C., Shuangshoti,S., Matangkasombut,O., and Mutirangura,A. (2008). Detection of LINE-1s hypomethylation in oral rinses of oral squamous cell carcinoma patients. Oral Oncol.

Thomson,P.J. (2002). Field change and oral cancer: new evidence for widespread carcinogenesis? Int. J. Oral Maxillofac. Surg. *31*, 262-266.

Uesugi,H., Uzawa,K., Kawasaki,K., Shimada,K., Moriya,T., Tada,A., Shiiba,M., and Tanzawa,H. (2005). Status of reduced expression and hypermethylation of the APC tumor suppressor gene in human oral squamous cell carcinoma. Int. J. Mol. Med. *15*, 597-602.

Vairaktaris,E., Yapijakis,C., Serefoglou,Z., Avgoustidis,D., Critselis,E., Spyridonidou,S., Vylliotis,A., Derka,S., Vassiliou,S., Nkenke,E., and Patsouris,E. (2008). Gene expression polymorphisms of interleukins-1 beta, -4, -6, -8, -10, and tumor necrosis factors-alpha, -beta: regression analysis of their effect upon oral squamous cell carcinoma. J. Cancer Res. Clin. Oncol. *134*, 821-832.

Viet,C.T. and Schmidt,B.L. (2008). Methylation array analysis of preoperative and postoperative saliva DNA in oral cancer patients. Cancer Epidemiol. Biomarkers Prev. *17*, 3603-3611.

Wang,Y.F., Chang,S.Y., Tai,S.K., Li,W.Y., and Wang,L.S. (2002). Clinical significance of interleukin-6 and interleukin-6 receptor expressions in oral squamous cell carcinoma. Head Neck *24*, 850-858.

Wehbe,H., Henson,R., Meng,F., Mize-Berge,J., and Patel,T. (2006). Interleukin-6 contributes to growth in cholangiocarcinoma cells by aberrant promoter methylation and gene expression. Cancer Res. *66*, 10517-10524.

Whiteside,T.L. (2009). Tricks tumors use to escape from immune control. Oral Oncol. *45*, e119-e123.

Yang,A.S., Estecio,M.R., Doshi,K., Kondo,Y., Tajara,E.H., and Issa,J.P. (2004). A simple method for estimating global DNA methylation using bisulfite PCR of repetitive DNA elements. Nucleic Acids Res. *32*, e38.

Yoo,C.B. and Jones,P.A. (2006). Epigenetic therapy of cancer: past, present and future. Nat. Rev. Drug Discov. *5*, 37-50.

Zhang,X., Guo,A., Yu,J., Possemato,A., Chen,Y., Zheng,W., Polakiewicz,R.D., Kinzler,K.W., Vogelstein,B., Velculescu,V.E., and Wang,Z.J. (2007). Identification of STAT3 as a substrate of receptor protein tyrosine phosphatase T. Proc. Natl. Acad. Sci. U. S. A *104*, 4060-4064.

7 Acknowledgements

8 Curriculum Vitae

Jacqueline Gasche

Birth Date/ Place   August 3rd, 1984 in Vienna, Austria

Nationality   Austria, Germany

Education

<u>University</u>

2002-2008   **Dental School at the University of Heidelberg, Germany**

04/2005   First State Examination

27.06.2008   Graduation with Award of Excellence

Since 2002   **Medical School at the University of Heidelberg, Germany**

08/2005   First State Examination

Since 2009   **Doctoral Thesis at the University of Tübingen, Germany**

„Chronic Inflammation of the Oral Cavity and Squamous Cell DNA Methylation" (J. Hoffmann, MD DMD PhD),

Division of Oral and Maxillofacial Surgery,

University Hospital Tübingen, Germany

01-02/2009   Christian-Doppler Cancer Research Lab (C. Gasche, MD PhD), Division of Gastroenterology,

Medical University of Vienna, Austria

Since 03/2009   G.I. Cancer Research Lab (C.R. Boland, MD PhD),

Division of Gastroenterology,

Baylor University Medical Center, Dallas, TX, USA

<u>School</u>

1994-1999	High School in Klosterneuburg, Austria
1999-2001	Torrey Pines High School, San Diego, CA, USA
2001-2002	High School in Klosterneuburg, Austria
05/2002	Graduation with Award of Excellence

Work Experience

07/2000	Training at the research laboratory, University of California, San Diego, USA (Lab: C.R. Boland, MD PhD)
2001-2002	Assistant in the medical practice (C. Gasche, MD PhD), Klosterneuburg, Austria
03/2006	Training at the research laboratory, Medical University Vienna, Austria (Lab: C. Gasche, MD PhD)
03/2007	Clinical clerkship at the University Hospital Vienna Division of Head and Neck Surgery, Austria

Honors and Awards

1994-1999	High School Klosterneuburg: outstanding achievements
1999-2001	Torrey Pines High School: grade point average of 4.4
2000	Physics Honors: Best Student Award
2000	Avocado League Basketball Champion
2001-2002	High School Klosterneuburg: outstanding achievements
2002	Austrian Basketball Champion (Team Vienna 87)
2002	Vienna City Basketball Champion (Team Vienna 87)
2002	High School Graduation: Award of Excellence (written diploma on „The Physics of Rollercoasters")
2008	University Graduation: Award of Excellence

9 Publication

At time of doctoral thesis submission, the manuscript of this project is in the process of preparation and submission to a cancer-related journal. As publication with first authorship is aspired, the author kindly asks to put the final grading decision on hold until acceptance from a journal. The author will keep the "Promotionsbüro" of the University of Tübingen informed of the publication status.